

Accepted Manuscript

Versatility of microglial bioenergetic machinery under starving conditions

Adam M. Nagy, Rebeka Fekete, Gergo Horvath, Gabor Koncsos, Csilla Kriston, Anna Sebestyen, Zoltan Giricz, Zsuzsanna Kornyei, Emilia Madarasz, Laszlo Tretter



PII: S0005-2728(17)30193-7

DOI: <https://doi.org/10.1016/j.bbabbio.2017.12.002>

Reference: BBABIO 47856

To appear in:

Received date: 5 September 2017

Revised date: 11 December 2017

Accepted date: 16 December 2017

Please cite this article as: Adam M. Nagy, Rebeka Fekete, Gergo Horvath, Gabor Koncsos, Csilla Kriston, Anna Sebestyen, Zoltan Giricz, Zsuzsanna Kornyei, Emilia Madarasz, Laszlo Tretter, Versatility of microglial bioenergetic machinery under starving conditions. The address for the corresponding author was captured as affiliation for all authors. Please check if appropriate. Bbabbio(2017), <https://doi.org/10.1016/j.bbabbio.2017.12.002>

This is a PDF file of an unedited manuscript that has been accepted for publication. As a service to our customers we are providing this early version of the manuscript. The manuscript will undergo copyediting, typesetting, and review of the resulting proof before it is published in its final form. Please note that during the production process errors may be discovered which could affect the content, and all legal disclaimers that apply to the journal pertain.

Title: Versatility of microglial bioenergetic machinery under starving conditions

Running title: Energy-donor substrates in starving microglia

Authors: Adam M. Nagy¹, Rebeka Fekete², Gergo Horvath¹, Gabor Koncsos³, Csilla Kriston⁴, Anna Sebestyen⁴, Zoltan Giricz³, Zsuzsanna Kornyei², Emilia Madarasz², Laszlo Tretter¹

¹ Department of Medical Biochemistry and MTA-SE Laboratory for Neurobiochemistry, Semmelweis University; 1094 Tuzolto st. 37-47, Budapest, Hungary

² Institute of Experimental Medicine of the Hungarian Academy of Sciences; 1083 Szigony st. 43, Budapest, Hungary

³ Department of Pharmacology and Pharmacotherapy, Semmelweis University; 1089 Nagyvarad square 4, Budapest, Hungary

⁴ 1st Department of Pathology and Experimental Cancer Research, Semmelweis University; 1085 Ulloi st. 26, Budapest, Hungary

Laboratory of origin: Department of Medical Biochemistry and MTA-SE Laboratory for Neurobiochemistry, Semmelweis University; 1094 Tuzolto st. 37-47, Budapest, Hungary

Correspondence:

Laszlo Tretter MD, PhD

Department of Medical Biochemistry, Semmelweis University

H-1094 Budapest, Tuzolto st 37-47, Hungary

Tel: + 36 1 459 1500 / ext. 60020

Fax: + 36 1 267 0031

Email: tretter.laszlo@med.semmelweis-univ.hu

Abstract

Microglia are highly dynamic cells in the brain. Their functional diversity and phenotypic versatility brought microglial energy metabolism into the focus of research. Although it is known that microenvironmental cues shape microglial phenotype, their bioenergetic response to local nutrient availability remains unclear.

In the present study effects of energy substrates on the oxidative and glycolytic metabolism of primary – and BV-2 microglial cells were investigated. Cellular oxygen consumption, glycolytic activity, the levels of intracellular ATP/ADP, autophagy, mTOR phosphorylation, apoptosis and cell viability were measured in the absence of nutrients or in the presence of physiological energy substrates: glutamine, glucose, lactate, pyruvate or ketone bodies.

All of the oxidative energy metabolites increased the rate of basal and maximal respiration. However, the addition of glucose decreased microglial oxidative metabolism and glycolytic activity was enhanced. Increased ATP/ADP ratio and cell viability, activation of the mTOR and reduction of autophagic activity were observed in glutamine-supplemented media. Moreover, moderate and transient oxidation of ketone bodies was highly enhanced by glutamine, suggesting that anaplerosis of the TCA-cycle could stimulate ketone body oxidation.

It is concluded that microglia show high metabolic plasticity and utilize a wide range of substrates. Among them glutamine is the most efficient metabolite. To our knowledge these data provide the first account of microglial direct metabolic response to nutrients under short-term starvation and demonstrate that microglia exhibit versatile metabolic machinery. Our finding that microglia have a distinct bioenergetic profile provides a critical foundation for specifying microglial contributions to brain energy metabolism.

Keywords

energy metabolism, mitochondria, glycolysis, glutamine, autophagy

Abbreviations

Artificial Cerebrospinal Fluid (ACSF), 3-hydroxybutyrate (BOHB), 2,4-dinitrophenol (DNP), carbonyl cyanide-*p*-trifluoromethoxyphenylhydrazone (FCCP), lactate dehydrogenase (LDH), phosphatidylethanolamine-conjugated LC3 (LC3 II), phosphatidylethanolamine-unconjugated LC3 (LC3 I)

1. Introduction

Microglia comprise a highly responsive population of cells with a key role in the regulation of the immune surveillance of the central nervous system (Sandiego *et al.* 2015, Kettenmann *et al.* 2011, Davalos *et al.* 2005). Aside from surveying the brain parenchyma, several other functions are implicated with respect to these cells (Michell-Robinson *et al.* 2015), including the control of neuronal death (Bessis *et al.* 2007), synaptic pruning (Paolicelli *et al.* 2011), regulation of neural circuits (Schafer *et al.* 2012, Miyamoto *et al.* 2016, Wake *et al.* 2009) or the induction of the reactive astroglial phenotype (Liddelow *et al.* 2017).

Microglia, even in the “resting” state, represent highly dynamic cell populations in the central nervous system. They exhibit heterogeneous shapes following morphological reorganization, which enables them to effectively control the microenvironment with extreme motile processes, engulf tissue components and clear metabolic products (Nimmerjahn *et al.* 2005). The maintenance of the phospholipid bilayer and the constant restructuring of the actin-microtubule cytoskeleton are assigned to a significant fraction of the brain's energy consumption (Engl *et al.* 2017). In order to meet this energy requirement at different regions of the brain, microglia must have a continuous supply of energy substrates and require versatile metabolic machinery. These cells express a range of transporters for the import of fuel metabolites that are potentially present as energy donors in the cerebrospinal fluid: glucose, glutamine, pyruvate, lactate and ketone bodies (Nijland *et al.* 2014, Schilling & Eder 2004, Zhang *et al.* 2014). This expression profile differs from that of other cells in the CNS and enables microglia to adapt various metabolic conditions upon migration.

In addition to microglial high dynamic activity and unique expression profile, their phenotypic diversity is also a key interest that brings microglial energy metabolism more into the focus of research. Recent papers revealed a link between microglial polarization states and energy metabolism (Voloboueva *et al.* 2013, Gimeno-Bayon *et al.* 2014, Orihuela *et al.* 2015). These studies reveal important findings exploring microglial energy metabolism, showing a shift from oxidative to glycolytic metabolism in response to activation signals. Recent work has demonstrated that microglia from aged mice have a change in energy metabolism, making a shift from glycolytic energy provision to fatty acid oxidation (Flowers *et al.* 2017). These studies reveal important findings about microglial energy metabolism, however they consider microglial metabolic microenvironment as a constant factor.

Microenvironmental regulatory factors define microglial transcriptional network and maintain regional specialization of microglial phenotypes in the CNS (Gosselin *et al.* 2017, Trenkmann

2017). Indeed, genes related to classical microglial cell processes, particularly cytoskeletal regulation and inflammatory signaling appear to be constitutively active, however, genes involved in mitochondrial function and cell metabolism are differentially expressed across brain regions (De Biase *et al.* 2017, Grabert *et al.* 2016). Despite intensive research in the field, key aspects of microglial bioenergetics have remained elusive.

Among the various cell types in the brain a close metabolic cooperation might exist. Glycolytic lactate is released from astrocytes and can be taken up by the neurons (Pellerin & Magistretti 1994, Dringen *et al.* 1993, Schurr *et al.* 1988). Neuronal glutamate is detoxified by astrocytes and the formed glutamine can be an energy source for neurons (Benjamin & Quastel 1974, Schousboe *et al.* 1992). On the other hand glutamate released from neurons could be an energy source for astrocytes (Schousboe *et al.* 1977). Astrocytes are able to produce ketone bodies that can be energy source of neurons (Blazquez *et al.* 1999). Neurons can release N-acetyl-aspartate and oligodendrocytes can utilize them (Chakraborty *et al.* 2001). Although microglial cells represent a high percentage of total cell number in the brain, yet the metabolic cooperation between microglia and other cells of the CNS remains incompletely understood.

The aim of this study therefore was to determine the potential substrates that support energy metabolism in starving microglial cells and to propose possible metabolic cooperations between microglia and other cell types in the CNS.

2. Materials and Methods

2.1 Materials

Unless otherwise indicated, all reagents were obtained from Sigma-Aldrich (St Louis, MO, USA). Glutamine was purchased from Merck KgaA (Darmstadt, Germany). Stock solutions of glutamine were prepared in bidistilled water, stored at -20°C and used only once after thawing to avoid degradation. For the assays, the medium was changed to artificial cerebrospinal fluid (ACSF) (145mM NaCl, 3 mM KCl, 2 mM CaCl₂, 1 mM MgCl₂, 10 mM HEPES; pH = 7.4).

2.2 Cell culture

BV-2 immortalized murine microglial cells (RRID:CVCL_0182), a kind gift from Prof. Rosario Donato (Department of Experimental Medicine and Biochemical Sciences, Perugia, Italy), were grown on Poly-L-lysine coated plastic tissue culture flasks in DMEM (Sigma D6546), supplemented with 4 mM glutamine, 10% FCS and 100 U/ml penicillin and 100 µg/ml streptomycin. This culture medium comprised the 'DMEM control' condition in all experiments.

Primary microglial cells were isolated from the forebrains of 1- to 2-day old CD1 mice according to (Saura *et al.* 2003). Both sexes of animals were included in the experiments; the ratio between male and female animals was 1:1. The animals were maintained and the experiments were performed in accordance with the Guidelines for Animal Experiments at Semmelweis University. The mice were euthanized via decapitation. Ten to thirteen animals were used per cell culture, resulting approximately 3×10^6 microglial cells at the end of the isolation. Primary microglia were co-cultured with astrocytes and were grown on Poly-L-lysine coated plastic tissue culture petri dishes in MEM (Sigma M2279), supplemented with 4 mM glutamine, 10% FCS and 100 U/ml penicillin and 100 µg/ml streptomycin. At 24-26 days after isolation, microglial cells were harvested as previously described (Saura *et al.* 2003).

2.3 Measurement of mitochondrial oxidation and glycolytic activity

The oxygen consumption rate (OCR, which reflects mitochondrial oxidation) and the extracellular acidification rate (ECAR, which is considered a parameter of glycolytic activity) were measured using a microfluorimetric Seahorse XF96 Analyzer (Agilent Technologies, USA) as previously described (Gerencser *et al.* 2009, Nemeth *et al.* 2015, Jady *et al.* 2016). Primary microglial cells were seeded 48 hours prior to the assays in Poly-L-lysine coated XF96 cell culture microplates (Seahorse Bioscience) at 4×10^4 cells/well density in 150 µl growth media. BV-2 cells were plated at

1.5×10^4 cells/well density in the same type of cell culture microplate 24 hours prior to the assays in 100 μ l growth media. Two hours prior to the assay, the growth medium was changed to 180 μ l ACSF assay medium. The O_2 tension and pH values were detected, and the oxygen consumption rates and extracellular acidification rates were calculated via XF96 Analyzer software (Agilent Technologies, USA). The basal rate of respiration corresponded to the last 30 minutes of the two-hour-long starvation in ACSF. Substrates (glucose 10 mM, glutamine 2.5 mM, pyruvate 5 mM, lactate 5 mM, 3-hydroxybutyrate 5 mM (BOHB), and acetoacetate 5 mM) or metabolic inhibitors/modulators (oligomycin 5 μ M, 2,4-dinitrophenol (DNP) 100 μ M or carbonyl cyanide-*p*-trifluoromethoxyphenylhydrazone (FCCP) 1.5 μ M as uncouplers, antimycin A 1 μ M, and sodium oxamate 10 mM), prepared in assay media, were injected into each well during the measurement. The concentrations of FCCP and oligomycin were titrated to obtain the maximal oxygen consumption/maximal inhibition, and the optimal 1.5 μ M/5 μ M were used in all experiments. DNP was also used in the measurements as an uncoupler instead of FCCP. No difference was identified between the effects of FCCP and DNP on the maximal respiration.

2.4 Measurement of intracellular ATP and ADP levels

The ATP and ADP levels were estimated using a Bioluminescent ATP assay kit (Biothema, Sweden). Measurements were performed on a Galaxy Bio-Orbit 1258 Microplate Luminometer in white luminescent microplates. Cell numbers were the same as described in the *Measurement of mitochondrial oxidation and glycolytic activity* subsection of the Materials and Methods part. On the day of the experiment, the cells were washed and incubated for two hours in ACSF medium (pre-warmed to 37°C). The ACSF was subsequently supplemented with the appropriate substrate (with the exception of in the control wells), and the cells were further incubated for two hours. This starvation protocol was followed in the other methods. Following four hours of incubation, the medium was changed to an ATP assay medium, and the extraction of ATP and ADP from the cells was immediately achieved with the addition of Extractant B/S (from Biothema). The ATP assay is based on the firefly luciferase reaction and was performed with a recombinant and thermostable luciferase according to (Lundin *et al.* 1986). The ATP and ATP+ADP assays were performed in two separate reaction mixtures. The measurements were performed in an ATP assay medium, which contained Tris 0.1 M, EDTA 2 mM, Potassium acetate 20 mM and phosphoenolpyruvate 1 mM. Pyruvate kinase 2 U/ml was added to the wells in which the ATP+ADP levels were detected. The assays were individually calibrated by measuring the light before and after the addition of a known amount of the BioThema certified and liquid-stable ATP standard.

2.5 Assessment of cell viability

The cell reduction capacity was measured using the MTT assay (3-(4,5-dimethylthiazol-2-yl)-2,5-diphenyltetrazolium bromide) and was considered a test for cell viability (Mosmann 1983). Cell numbers were the same as described in the *Measurement of mitochondrial oxidation and glycolytic activity* subsection of the Materials and Methods part. The incubation time and substrate conditions were the same as described for the ATP/ADP measurements: microglial cells were washed and incubated in nutrient-free ACSF for two hours; they were further incubated for two hours in ACSF assay medium, which was supplemented with a single substrate (with the exception of the ACSF controls). After four hours of incubation, MTT reagent was added, and the cells were further incubated at 37°C for one hour. The converted dye was subsequently solubilized by the addition of acidic isopropanol (0.04 M HCl in absolute isopropanol), and the absorbance intensity of $\lambda = 570$ nm light (proportional to the formazan concentration in the solution) was measured.

2.6 Apoptosis/necrosis assay

Apoptotic cells were detected using Annexin V – Cy3.18 (Vermes *et al.* 1995). The cell permeability was tested by the acethoxymethyl-calcein ester (calcein-AM; Invitrogen) method (Bozyczko-Coyne *et al.* 1993). 3×10^5 cells were seeded onto Poly-L-lysine coated glass coverslips. Prior to the annexin and calcein stainings, the cells were washed twice with ACSF, followed by incubation in ACSF that contained various substrates, at 37°C, with no CO₂ supplementation. The incubation times in the ACSF and substrate concentrations were the same as described in the other methods: two hours of starvation was followed by two hours of incubation in substrate-supplemented media (with the exception of the ACSF controls). The microglial cells were subsequently stained with Annexin-V according to the manufacturer's instructions. Briefly, the cells were incubated with 1 μ g/ml Annexin V. Cy3.18 (Sigma A4963) for 10 min at room temperature. The cells were simultaneously loaded with 1 μ g/ml calcein-AM for 10 minutes at room temperature. After repeated washing steps live cells were immediately analyzed by a Zeiss Axiovert 200M microscope. The number of calcein and Annexin V positive cells were determined manually on images taken with a 10x EC plan-Neofluar objective, using Zeiss filter sets 20 and 38HE. The presented data are obtained from 4-4 experimental series (primary microglia and BV2 cells, n=3 for parallel cultures in each condition, 6-8 image from each culture). Cells stained only with calcein were considered vital cells. The Annexin-V labelled cells were considered necrotic, and the double stained cells comprised apoptotic cells.

2.7 Western blot

BV-2 microglial cells were seeded onto Poly-L-lysine coated 6-well tissue culture plates at 3×10^5 cells/well density. On the day of the experiment, the same starvation protocol was used as described in the other methods: two hours of incubation of the cells in nutrient-free ACSF was followed by an additional two-hour long incubation with a single substrate (with the exception of the ACSF controls). The cells were subsequently homogenized in RIPA lysis buffer (Thermo Fisher Scientific, Waltham, MA, US), supplemented with protease inhibitor (Roche, Basel, Switzerland) and PMSF (Sigma, St. Louis, MO, US). A Bicinchonic Acid Assay kit (Thermo Fisher Scientific, Waltham, MA, US) was used to measure the protein concentration of the lysates. Approximately 12-16 μg of protein from each lysate were mixed with reducing 5 \times Laemmli buffer, loaded and separated in a 4–20 % precast Tris–glycine SDS polyacrylamide gel (Bio-Rad, Hercules, CA, US). The separated proteins were transferred to a polyvinylidene difluoride membrane (Bio-Rad, Hercules, CA, US) at 350 mA for 2 hours. Visualization of proper transfer was assessed via Ponceau S staining (Sigma, St. Louis, MO, US). The blockade of non-specific binding was conducted with 5% non-fat milk (Bio-Rad, Hercules, CA, US) or BSA (Santa Cruz Biotechnology, Dallas, TX, US) in Tris-buffered saline that contained 0.05 % Tween-20 (0.05% TBS-T; Sigma, St. Louis, MO, US) at room temperature for two hours. Immunoblotting was performed as recommended by the antibody manufacturers. The primary antibodies (marker of autophagy: microtubule-associated protein 1 light chain 3 II/I [LC3 II/I]—#4108; markers of mTOR pathway: phospho-mTOR [Ser2448]—#2971; mTOR—#2972, phospho-AMP-activated protein kinase α [AMPK α ; Thr172]—#2535; AMPK α —#5831) were purchased from Cell Signaling (Danvers, MA, US). Immunoreactivity was detected with the corresponding horseradish peroxidase-conjugated secondary antibody (Cell Signaling, Danvers, MA, US) for 2 h at room temperature. The signals were detected with an enhanced chemiluminescence detection reagent (Bio-Rad, Hercules, CA, US) by Chemidoc XRS+ (Bio-Rad, Hercules, CA, US). For the removal of antibodies that detected phosphorylated epitopes, Pierce Stripping Buffer (Thermo Fisher Scientific, Waltham, MA, US) was used prior to incubation with antibodies that detected the total protein.

2.8 Flow cytometry

BV-2 microglial cells were incubated in nutrient-free ACSF for two hours; the ACSF assay medium was subsequently supplemented with a single substrate (with the exception of the ACSF controls) in the same way as described in the other methods. For the p-S6 expression analysis, 5×10^5 cells/condition were stained using the PerFix-nc Kit (Beckman Coulter) following the manufacturer's instructions. The p-S6 expression was detected with direct-labelled monoclonal p-

S6 antibody (Cell Signaling #5316). The samples were measured on a Navios flow cytometer (Beckman Coulter) and analysed using Kaluza software (Beckman Coulter).

2.9 Statistical Analysis

Data were pooled from a minimum of three individual experiments and are presented as the mean \pm SEM. Significant differences between multiple groups were determined via one-way ANOVA and ANOVA on ranks was used, when the normality assumption has been violated. Individually determined *p* values are presented in Figure legends. Statistical analyses were performed using the Sigmaplot Systat software (RRID:SCR_003210).

ACCEPTED MANUSCRIPT

3. Results

3.1 Effects of energy substrates on cellular respiration and glycolytic activity

3.1.1 Effect of single substrates on cellular respiration and glycolytic activity

The measurement of the oxygen consumption of intact, adherent cells is one of the most direct, dynamic methods to quantify *in situ* mitochondrial function. In this study, the effects of different energy substrates, which may be present in the CSF, on the cellular respiration of primary and BV-2 microglia were investigated using a Seahorse XF96 Extracellular Flux Analyzer and the summary of the data is presented in Table 1A and 1B. The values are expressed as a percentage of the basal level of respiration measured in the absence of metabolic fuels. It is important to note that in 30 minutes, the respiratory rate of primary microglia was decreased to 89.76 ± 1.08 % and to 85.29 ± 0.85 % by the BV-2 cells following starvation in ACSF in the absence of exogenous energy donor substrates (Fig. 1 and Table 1, Row b). Thus, BV-2 cells were slightly more sensitive to starvation compared with primary microglial cells. To determine the oxygen consumption associated with ATP synthesis, the mitochondrial F_1F_0 - ATP synthase was inhibited with oligomycin, which resulted in a decrease in the mitochondrial oxygen consumption (Table 1, Row c). The part of respiration used for oxidative phosphorylation was calculated from *i*) the oxygen consumption measured in the presence of substrate (*b*) and *ii*) the oxygen consumption measured in the presence of an ATP-synthase inhibitor (*c*) using formula (*b-c*).

Maximal respiration may be elicited by the addition of the protonophore FCCP, which induces the collapse of the mitochondrial membrane potential. In the presence of FCCP, the mitochondrial electron transport chain may operate without the limitation of respiration by the high electrochemical proton gradient across the inner mitochondrial membrane. Thus, uncoupling the oxidative phosphorylation with FCCP enables the determination of the maximal respiration, which may be limited by the substrate supply. The small response of starving cells to FCCP demonstrates the limited substrate supply (Table 1, Row d). In this condition, cells may only rely on endogenous reserve substrates, potentially amino acids, derived from proteolysis, and fatty acids. Uncoupler on one hand stimulates the respiration, but on the other hand this stimulation accelerates the consumption of reserves, thus the transient stimulation is followed by a fast decay. To address the contribution of fatty acids in the respiration of starving cells, Etomoxir was added to inhibit the mitochondrial long-chain fatty acid transporter CPT-1. A decline was observed in mitochondrial oxygen consumption upon the injection of the inhibitor (data not shown), which may reflect the utilization of endogenous lipids, but other off-target effects are also related to Etomoxir.

Fig. 1.

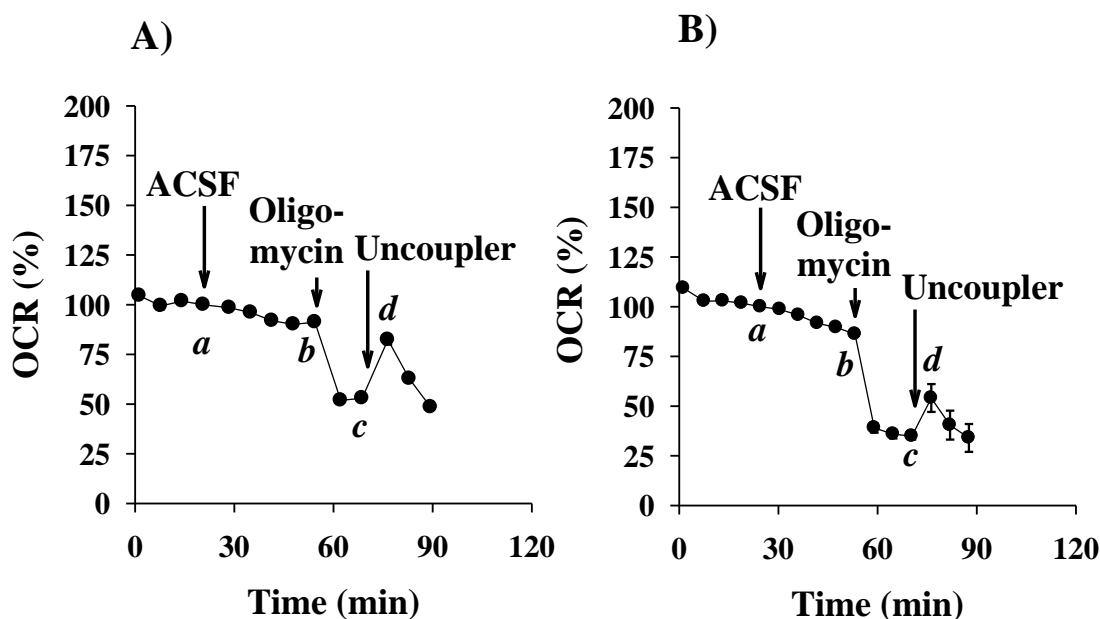


Fig. 1. Representative curves of oxygen consumption rates measured in primary (A) - and BV-2 (B) microglial cells in the absence of additional substrate. Starving conditions were as described in Materials and Methods. Respiratory variables are as indicated in Table 1A and 1B (Column: ACSF control): basal respiration (a); respiration with(out) substrate (b); respiration remaining after the inhibition of ATP-synthase (c). Data show the average values of 8-12 parallel wells \pm SEM. Abbreviations: OCR (Oxygen Consumption Rate), ACSF (Artificial Cerebrospinal Fluid)

Glucose is considered a primary energy source of the brain. A decrease was identified in the basal level of oxygen consumption by primary and BV-2 cells (69.88 ± 4.38 and 61.41 ± 1.07 , respectively) following the addition of glucose; these findings suggest that after two hours of starvation, exogenously added glucose reduces the mitochondrial respiration of microglial cells. The portion of oxygen consumption that is coupled to ATP synthesis was significantly decreased in the glucose-supplied compared with control starving cells (22.29 ± 1.27 versus 35.84 ± 1.31 in primary cells). However, the maximal respiration, elicited by the addition of FCCP, was significantly increased in the primary and BV-2 cells (111.81 ± 5.35 and 80.44 ± 5.29 , respectively) compared with the cells starving in ACSF (Table 1A and 1B, Row d). Similarly, the reserve respiration (the difference between the maximal (uncoupler stimulated) respiration and the respiration measured in the presence of substrate) was elevated in the presence of glucose by 41.9 ± 3.0 % in primary microglial cells and by 19.0 ± 5.0 % in BV-2 cells.

Parallel with the measurement of cellular respiration, the change in the pH in the ACSF was detected and considered a parameter of the glycolytic activity. The basal rate of acidification (100 %) was equal to 1.5 mpH/min/40,000 cell extracellular acidification rate by primary cultures of microglia and to 4.0 mpH/min/15,000 cell extracellular acidification rate by BV-2 cells. Glycolytic activity was markedly increased in the primary microglial cells and in the BV-2 microglial cells following the addition of glucose (Fig. 2B and 2D); these findings indicate that pyruvate produced in glycolysis is mainly converted to lactate instead of being oxidized by mitochondria. As expected, this high rate of acidification slowed down after the addition of sodium oxamate (10 mM), an inhibitor of lactate dehydrogenase (LDH). Oxamate reduced the glycolytic rate of the primary microglia from 500 % to 250 %, whereas in the BV-2 cells a complete block of lactate production was observed (Fig. 2B and 2D). Uncoupling the mitochondrial oxidative phosphorylation with FCCP resulted in an increase in acidification; the rate of which was decreased upon addition of the mitochondrial complex III inhibitor, antimycin (Fig. 2B and 2D). Oxamate addition provoked a slight increase in the cellular respiration as well as in the maximal respiration (Fig. 2A and 2C).

Fig. 2.

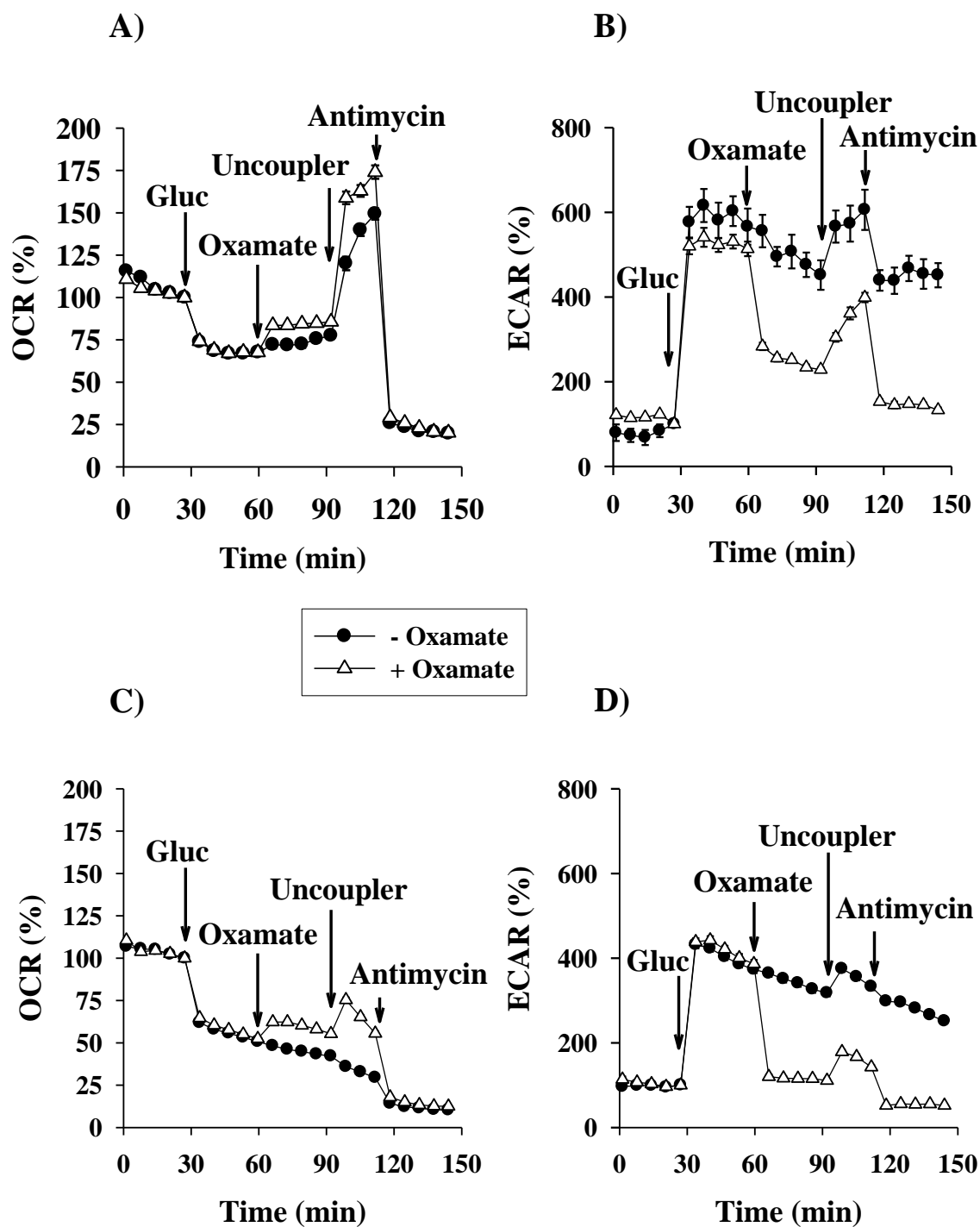


Fig. 2. Effect of lactate dehydrogenase inhibitor sodium oxamate on mitochondrial oxygen consumption and on glycolytic activity measured in primary (A, B) - and BV-2 (C, D) microglial cells in the presence of glucose. Starving conditions were as described in Materials and Methods. Metabolic inhibitors were given as indicated on Figures. Data points were obtained from 3 independent experiments and represent the mean values of 8-12 parallel wells \pm SEM. Abbreviations: OCR (Oxygen Consumption Rate), ECAR (Extracellular Acidification Rate), Gluc (Glucose)

Glutamine is abundantly present in the brain; its concentration in the CSF is one order of magnitude higher than that of other amino acids (Albrecht *et al.* 2007, McGale *et al.* 1977). Following transport through the cell membrane and mitochondrial inner membrane, in two steps, glutamine is converted to α -ketoglutarate, which may subsequently enter the TCA-cycle and contribute to the energy provision. The accumulation of ammonium in mitochondria may induce apoptosis in microglial cells when glutamine is present in increased concentrations in the cellular medium (Svoboda & Kerschbaum 2009). To avoid ammonium toxicity, a more physiologic 2.5 mM concentration of glutamine was used in our experiments and no reduction in the cell viability was identified (see later in Fig. 7). In the present study, the addition of glutamine after two hours of starvation slightly increased the basal respiration of primary and BV-2 microglial cells (115.39 ± 6.05 % and 121.54 ± 3.78 %, respectively). After the inhibition of glutamine-driven ATP synthesis with oligomycin, the percentage of remaining respiration (48.79 ± 1.42 %) was significantly increased compared with the starving control oxygen consumption (37.55 ± 0.75 %) in the BV-2 cells. This respiration may reflect the membrane potential dependent transport mechanisms through the inner mitochondrial membrane. The maximal respiration achieved by the addition of FCCP was significantly increased in the glutamine-supported primary and BV-2 microglial cells (148.62 ± 4.14 and 131.57 ± 5.19 , respectively). The reserve respiration capacity was stimulated upon adding glutamine as an exogenous substrate by 33.2 ± 5.0 % in primary microglia and by 10.0 ± 3.2 % in BV-2 cell line.

A 2 mpH/min increase in the extracellular acidification was identified in the presence of glutamine following the addition of the uncoupler. The respiratory complex III inhibitor Antimycin A decreased this acidification, which may reflect that the uncoupler mediated acidification was a consequence of an increased rate of oxidative decarboxylation during glutamine metabolism (Fig. 3B and 3D).

Fig. 3.

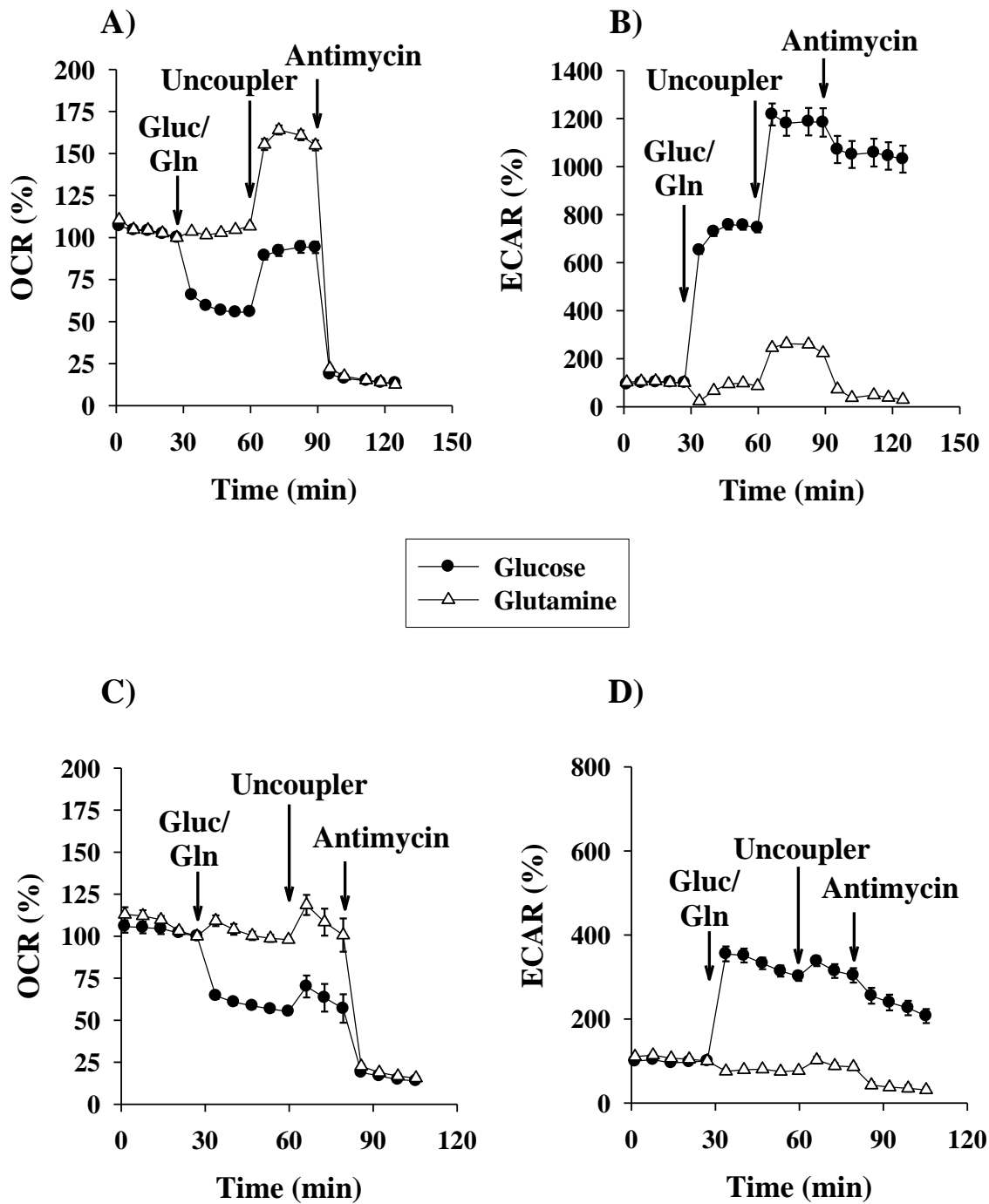


Fig. 3. Effect of glutamine and glucose on mitochondrial oxygen consumption and on glycolytic activity measured in primary (A, B) - and BV-2 (C, D) microglial cells upon starvation. Starving conditions were as described in Materials and Methods. Additions were as shown on Figures. Data are pooled at least from 3 independent cell culture preparations and show the average values of 8-12 parallel wells \pm SEM. Abbreviations: OCR (Oxygen Consumption Rate), ECAR (Extracellular Acidification Rate), Gluc (Glucose), Gln (Glutamine)

Pyruvate may serve as a potential energy substrate in the central nervous system (Peng *et al.* 1994). In this study, the basal level of respiration was increased by the addition of pyruvate, which was more pronounced in the primary cultures of microglia (118.23 ± 5.65 %) compared with the BV-2 cells (91.78 ± 3.26 %). The uncoupler mediated stimulation of respiration was the most pronounced in the presence of pyruvate in the primary microglia and was the second highest to glutamine in the BV-2 cells (Table 1A and 1B, Row d). The reserve respiration was increased by 46.3 ± 3.0 % in primary microglia (Table 1A, Rows (d-b)).

Lactate comprises another important energy metabolite in the CSF; it is proposed to be an oxidative substrate for neurons and oligodendrocytes (Rinholm & Bergersen 2014, Magistretti & Allaman 2015), whereas its contribution to microglial energy metabolism is yet unknown. We found a significant stimulation of basal respiration following the addition of lactate in the primary cultures of microglia and BV-2 cells (105.32 ± 2.05 % and 95.97 ± 3.10 %, respectively) compared with the ACSF control (89.76 ± 1.08 and 85.29 ± 0.85 , respectively). The extent of inhibition by oligomycin indicates that approximately 50% of the respiration is associated with ATP synthesis (Table 1A and 1B, Row c). However, the respiration driving ATP synthesis was very low with lactate in the primary cells (49.84 ± 1.67). The administration of the uncoupler FCCP significantly augmented the rate of oxidation in both the primary and BV-2 microglial cells (133.37 ± 3.37 % and 93.39 ± 5.69 %, respectively) compared with the ACSF control cells (Table 1A and 1B, Row d).

Ketone bodies may serve as alternative fuels for cells in the brain under energy-deprived conditions (Izumi *et al.* 1998, Owen *et al.* 1967). Beta-hydroxybutyrate (BOHB) is a ketone body that is converted to acetoacetate and subsequently to acetoacetyl-CoA, thereby forming two acetyl-CoA molecules that may enter into the TCA-cycle. The addition of BOHB after two hours of starvation resulted in a small and significant increase in the mitochondrial oxidation identified in primary and BV-2 cells (106.57 ± 2.50 and 98.86 ± 2.10 %, respectively) compared with the ACSF control (89.76 ± 1.08 and 85.29 ± 0.85 , respectively). In the primary cultures of microglia, the oxygen consumption driving ATP synthesis was high with BOHB (56.61 ± 2.18 %). Upon addition of FCCP maximal respiration hardly reached basal level in the primary microglia (108.24 ± 5.21) (Table 1A, Row d). Reserve respiratory capacity with BOHB was near to zero in primary microglia, but with BV-2 cells it was negative (-17.0 ± 5.5), i.e. respiration after uncoupler addition was lower than that immediately after substrate addition (Table 1A and 1B, Rows (d-b)).

3.1.2 Effect of substrate combinations on cellular respiration and glycolytic activity

Combination of acetoacetate and glutamine

In the first metabolic step in BOHB utilization, acetoacetate is produced, which is further metabolized in the presence of glutamine. The effects of acetoacetate supplementation on the uncoupled rate of oxygen consumption by primary and BV-2 cells in the presence of glutamine are presented in Fig. 4A and 4B. The maximal respiration reached by the addition of DNP was significantly smaller in the absence of acetoacetate than that with the glutamine plus acetoacetate. The addition of acetoacetate stimulated the uncoupler-mediated respiration by 160 % in the primary cells and 120 % in the BV-2 cells when glutamine was present in the media. Similar acceleration of uncoupler-mediated oxygen consumption was detected when BOHB was applied instead of acetoacetate (data not shown).

ACCEPTED MANUSCRIPT

Fig. 4.

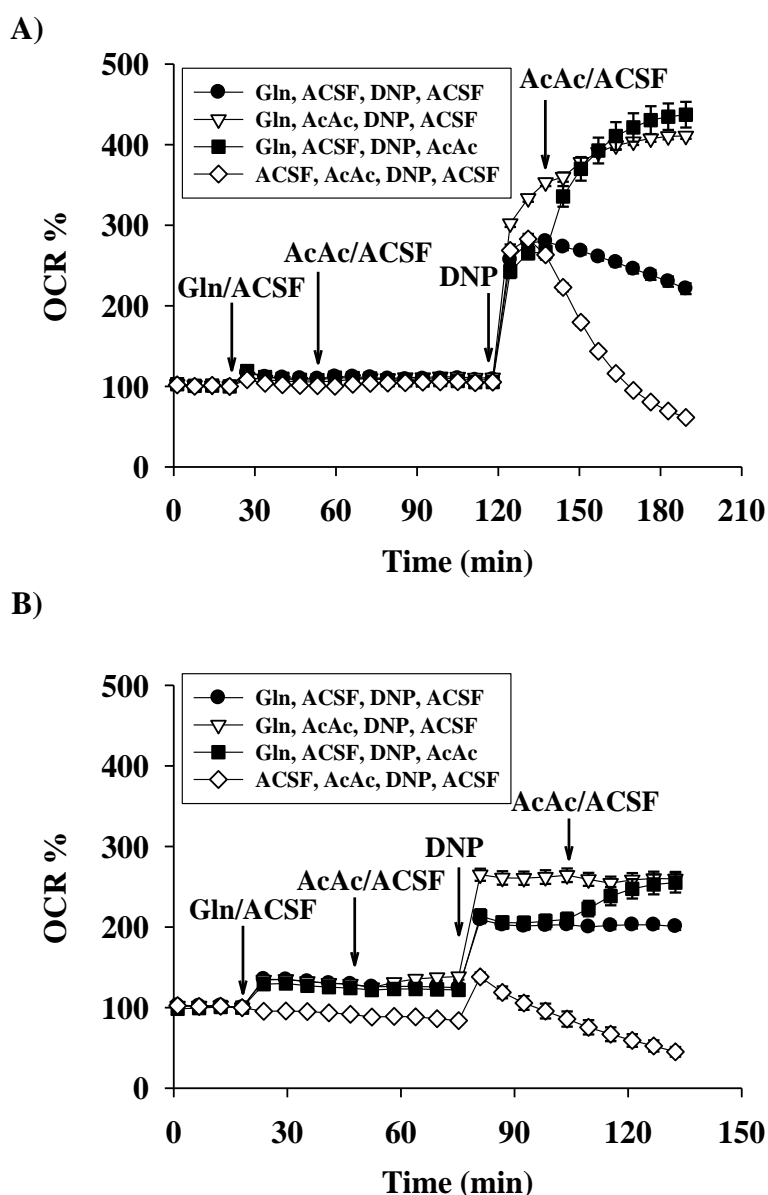


Fig. 4. Effect of acetoacetate on glutamine-driven respiration measured in primary (A) - and BV-2 (B) microglial cells after starvation. Starving conditions were as described in Materials and Methods. Additions were as shown on Figures. Abbreviations: OCR (Oxygen Consumption Rate), ECAR (Extracellular Acidification Rate), Gluc (Glucose), Gln (Glutamine), ACSF (Artificial Cerebrospinal Fluid), AcAc (Acetoacetate), DNP (2,4-dinitrophenol)

Combination of malate or aspartate with substrates contributing to acetyl-CoA formation (glucose, pyruvate or lactate)

Results presented above with substrate combination (glutamine plus oxaloacetate) underline the importance of anaplerosis in starving cells. In further experiments malate or aspartate were used as

possible anaplerotic substrates for the citrate synthase reaction. In order to investigate their anaplerotic capacity ACSF, or glucose, or pyruvate or lactate were added as “test” substrates. Only the aspartate pre-treatment was able to induce significant changes in maximal respiration with all the four test substrates used. In the presence of malate, a significant change in the maximal respiration was detected only with the glucose test substrate (Fig. 5. A-D).

ACCEPTED MANUSCRIPT

Fig. 5.

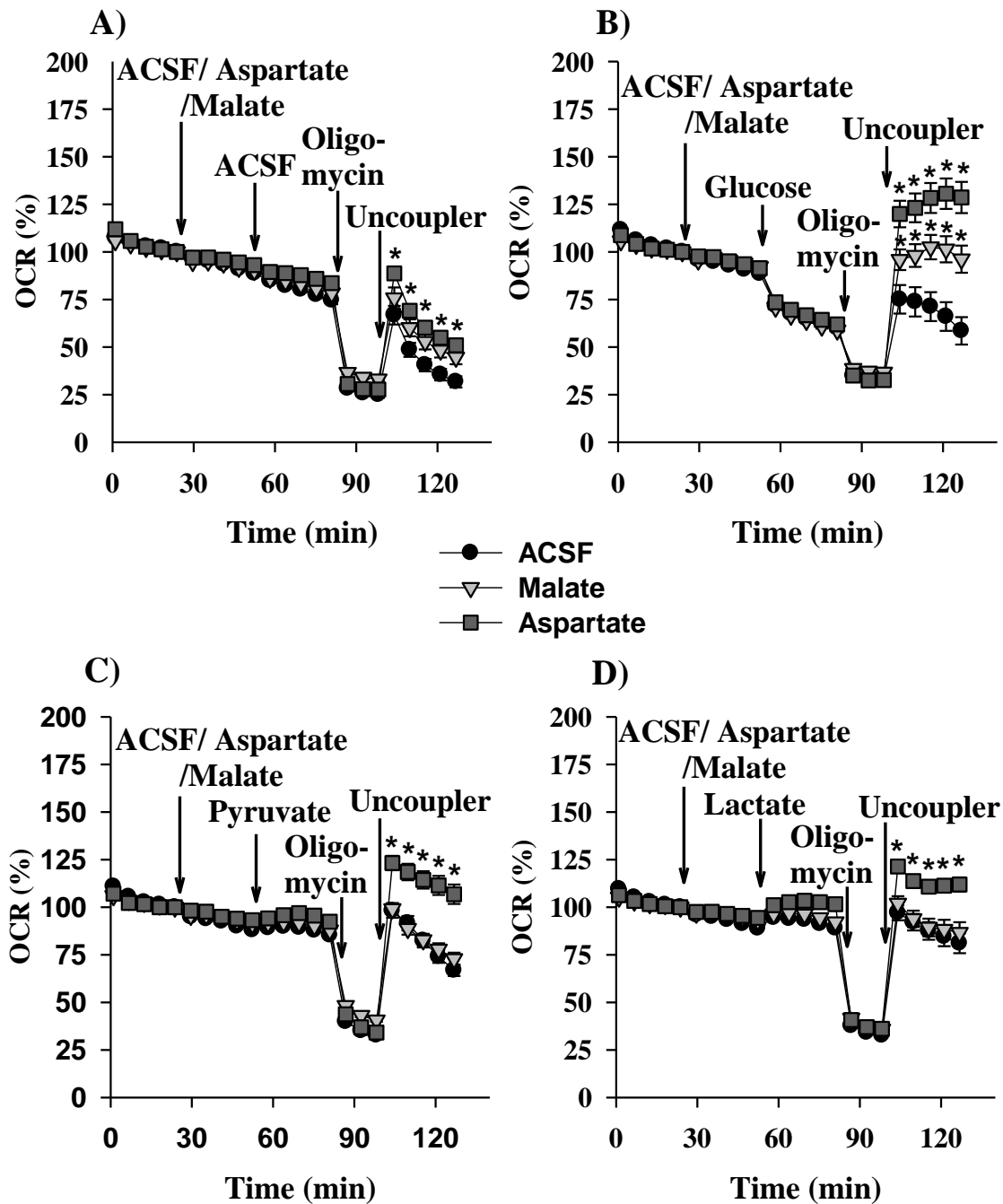


Fig. 5. Effect of aspartate and malate on starving (A), glucose - (B), pyruvate - (C) and lactate - driven respiration of BV-2 microglial cells. Starving conditions were as described in Materials and Methods. Additions were as shown on Figures. Data are pooled at least from 3 independent cell culture preparations and show the average values of 12-15 parallel wells \pm SEM. Abbreviations: OCR (Oxygen Consumption Rate), ACSF (Artificial Cerebrospinal Fluid)

Table 1.

A) Oxygen consumption % of primary microglial cells

%	<i>ACSF control</i> <i>N=133</i>	<i>Glucose</i> <i>N=34</i>	<i>Glutamine</i> <i>N=34</i>	<i>Pyruvate</i> <i>N=40</i>	<i>Lactate</i> <i>N=41</i>	<i>BOHB</i> <i>N=38</i>
<i>ACSF baseline (a)</i>	100.00 ± 4.41	100.00 ± 8.88	100.00 ± 8.06	100.00 ± 7.62	100.00 ± 6.81	100.00 ± 7.05
<i>Respiration with substrate (b)</i>	89.76 ± 1.08	69.88 ± 4.38	115.39 ± 6.05	118.23 ± 5.65	105.32 ± 2.05	106.57 ± 2.50
<i>Resp. after addition of oligomycin (c)</i>	53.92 ± 0.64	47.59 ± 3.60	59.74 ± 4.28	58.59 ± 4.14	55.48 ± 2.62	49.96 ± 3.19
<i>Maximal resp. (d)</i>	83.29 ± 3.02	111.81 ± 5.35	148.62 ± 4.14	164.48 ± 5.91	133.37 ± 3.37	108.24 ± 5.21
<i>Resp. driving ATP synth. (b-c)</i>	35.84 ± 1.31	22.29 ± 1.27	55.65 ± 2.62	59.64 ± 3.06	49.84 ± 1.67	56.61 ± 2.18
<i>Reserve respiratory capacity (d-b)</i>	-6.47 ± 2.27	41.93 ± 3.00	33.23 ± 5.02	46.25 ± 3.03	28.05 ± 4.92	1.67 ± 7.14

B) Oxygen consumption % of BV-2 microglial cells

%	<i>ACSF control</i> <i>N=116</i>	<i>Glucose</i> <i>N=50</i>	<i>Glutamine</i> <i>N=76</i>	<i>Pyruvate</i> <i>N=37</i>	<i>Lactate</i> <i>N=31</i>	<i>BOHB</i> <i>N=26</i>
<i>ACSF baseline (a)</i>	100.00 ± 4.46	100.00 ± 6.67	100.00 ± 5.59	100.00 ± 6.55	100.00 ± 6.94	100.00 ± 7.93
<i>Respiration with substrate (b)</i>	85.29 ± 0.85	61.41 ± 1.07	121.54 ± 3.78	91.78 ± 3.26	95.97 ± 3.10	98.86 ± 2.10
<i>Resp. after addition of oligomycin (c)</i>	37.55 ± 0.75	37.51 ± 0.87	48.79 ± 1.42	40.00 ± 1.29	40.62 ± 1.76	44.38 ± 1.56
<i>Maximal resp. (d)</i>	54.04 ± 2.45	80.44 ± 5.29	131.57 ± 5.19	95.15 ± 5.29	93.39 ± 5.69	81.86 ± 4.43
<i>Resp. driving ATP synth. (b-c)</i>	47.73 ± 0.93	23.90 ± 0.85	72.75 ± 2.58	51.78 ± 2.51	55.36 ± 2.78	54.48 ± 1.86
<i>Reserve respiratory capacity (d-b)</i>	-31.25 ± 2.10	19.03 ± 5.03	10.03 ± 3.18	3.37 ± 4.97	-2.58 ± 4.80	-17.00 ± 5.51

Table 1. Respiratory variables obtained with primary - (A) and BV-2 (B) microglial cells using different substrates. ACSF baseline was measured after two hours of incubation in ACSF without any addition of substrates. After starvation glucose, glutamine, pyruvate, lactate or BOHB was added except control wells. Respiratory variables: (a) basal respiration (average value of measurements before the addition of substrate); (b) respiration with substrate (average value of measurements prior to the addition of metabolic inhibitors); (c) respiration remaining after the inhibition of ATP-synthase (average value of measurements after the addition of oligomycin); (d) maximal respiration (average value of measurements after the addition of FCCP); (b-c) respiration driving ATP synthesis; reserve respiratory capacity (d-b). Data are expressed as % of control (ACSF baseline) and means ± SEM. Cells highlighted with black shading indicate statistically significant difference ($P < 0.05$) versus ACSF control evaluated by one-way ANOVA. 100 % was equal to 94.98 ± 2.58 pmol/min/40,000 cell oxygen consumption by primary cultures of microglia and to 160.82 ± 4.05 pmol/min/15,000 cell oxygen consumption by BV-2 cells. Data are pooled from minimum 3 independent cell culture preparations. *N* reflects the number of analyzed microcultures.

Table 2.

A) Oxygen consumption % of primary microglial cells

%	ACSF control N=133	Glucose N=34	Glutamine N=34	Pyruvate N=40	Lactate N=41	BOHB N=38
ACSF baseline (a)	100.00 ± 4.41	100.00 ± 8.88	100.00 ± 8.06	100.00 ± 7.62	100.00 ± 6.81	100.00 ± 7.05
Respiration with substrate (b)	89.76 ± 1.08	-19.88	+25.63	+28.47	15.56	16.81
Resp. after addition of oligomycin (c)	53.92 ± 0.64	-6.33	+5.82	+4.67	+1.56	-3.96
Maximal resp. (d)	83.29 ± 3.02	+28.52	+65.33	+81.19	+50.07	+24.95
Reserve respiratory capacity (d-b)	-6.47 ± 2.27	+48.4	+39.7	+52.72	34.52	+8.14

B) Oxygen consumption % of BV-2 microglial cells

%	ACSF control N=116	Glucose N=50	Glutamine N=76	Pyruvate N=37	Lactate N=31	BOHB N=26
ACSF baseline (a)	100.00 ± 4.46	100.00 ± 6.67	100.00 ± 5.59	100.00 ± 6.55	100.00 ± 6.94	100.00 ± 7.93
Respiration with substrate (b)	85.29 ± 0.85	-23.88	+36.25	+6.49	+10.68	+13.57
Resp. after addition of oligomycin (c)	37.55 ± 0.75	-0.04	+11.24	+2.45	+3.07	+6.83
Maximal resp. (d)	54.04 ± 2.45	+26.4	+77.53	+41.11	+39.35	+27.82
Reserve respiratory capacity (d-b)	-31.25 ± 2.10	+50.28	+41.28	+34.62	+28.67	+14.25

Table 2. was created from data of Table 1A and 1B. In every row corresponding ACSF control values were subtracted from ACSF plus substrate rates.

3.2 Effects of energy substrates on the intracellular ATP and ADP levels

The intracellular ATP and ADP levels were also determined following the incubation of cells with a single glycolytic or oxidative substrate for two hours. Prior to substrate addition starvation was induced as described in Materials and Methods, which substantially decreased the ATP levels both in the primary microglial cells and in the BV-2 (the cellular ATP content of the ACSF control cells compared with the MEM and DMEM controls, respectively). Fig. 6A demonstrates that all substrates added to ACSF were utilized effectively by primary microglial cells to maintain their cellular ATP content, which was higher than that in the absence of substrates. All substrates increased the ATP/ADP ratio in the primary cells compared with the ACSF controls. However, the effects of the substrates on the ATP levels were different in the BV-2 cells; in the presence of glutamine, the BV-2 cells maintained their intracellular ATP and ADP contents at the same levels as the DMEM control cells. In the presence of glucose, pyruvate, lactate and BOHB, the amount of cellular ATP decreased to the same level as the ACSF controls, whereas the ADP content was unaffected (Fig. 6B).

Fig. 6.

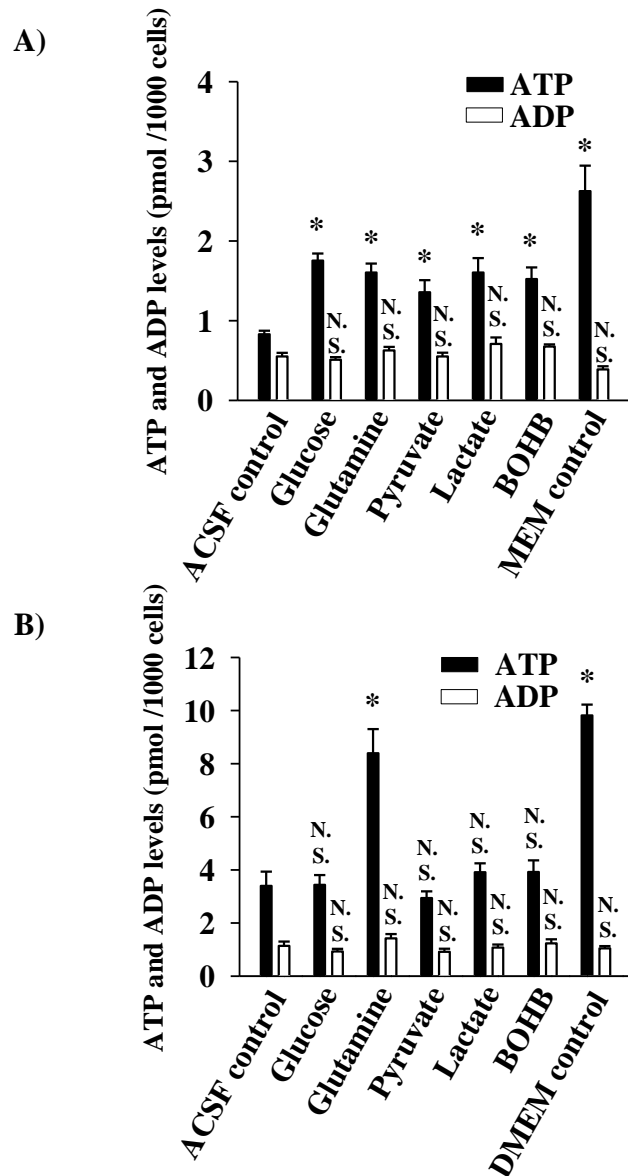


Fig. 6. Effect of energy substrates on the intracellular ATP and ADP levels in primary (A) - and BV-2 (B) microglial cells after starvation. Experimental conditions were as described in Materials and Methods. For starving control, microglial cells were incubated in nutrition-free ACSF. MEM and DMEM indicate conditions, where cells were incubated in culture media. Values represent the means \pm SEM for at least 3 independent experiments each with 6-8 replicate wells. * $P = <0,001$ indicate statistically significant difference versus ACSF control evaluated by one-way ANOVA.

3.3 Effect of energy substrates on cell viability

In the ACSF control condition, starvation had a major impact on the cell viability. In the present study, an MTT test was used to assess cell survival. The amount of formazan crystals, as a result of

MTT reduction by dehydrogenase enzymes in the cell, was proportional to the number of metabolically active microglial cells. Fig. 7A indicates that the viability of the primary microglial cells was not significantly decreased after starvation, and only slight differences were identified between the effects of substrates on the MTT viability. A substantially reduced MTT level was identified in the BV-2 cells after starvation. However, in the presence of glutamine, which was applied as a single substrate in the ACSF, a significantly increased MTT level was identified compared with the BV-2 cells starving in substrate-free ACSF medium (ACSF control); these findings suggest that glutamine replenishes the TCA-cycle to maintain the cell viability and fulfil the high energy need of the cell (Fig. 7B).

Fig. 7.

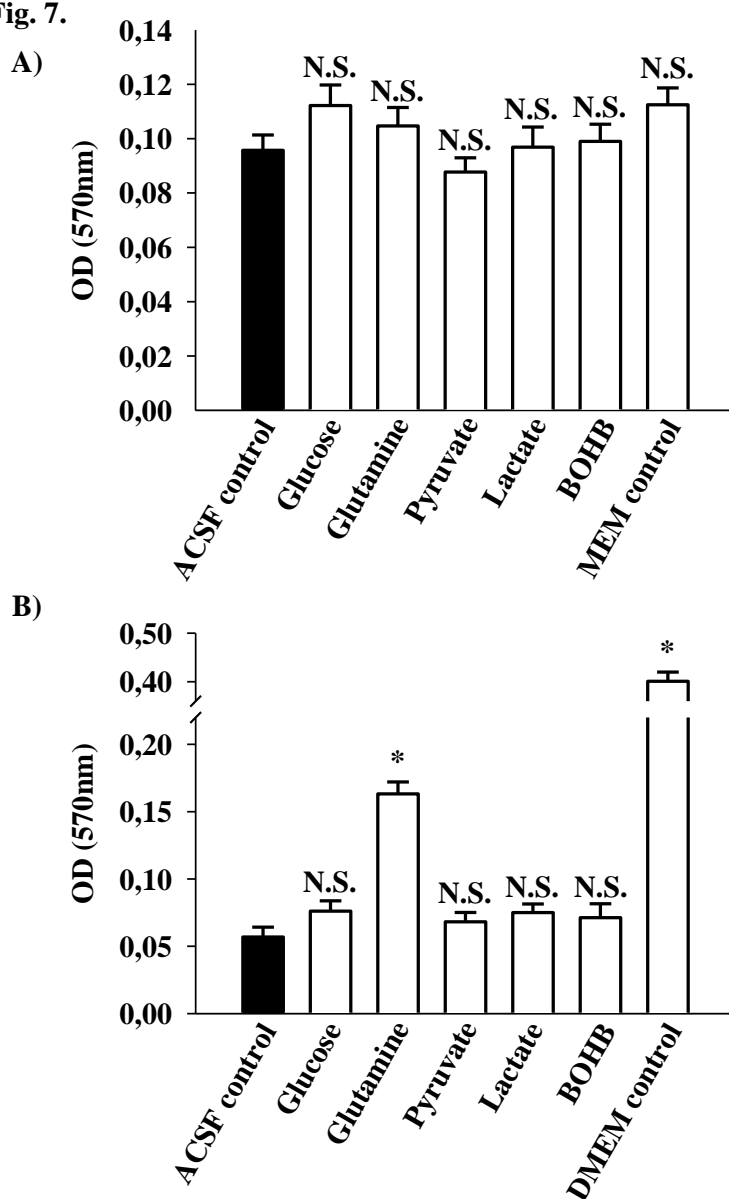


Fig. 7. MTT reduction capacity of primary (A) - and BV-2 (B) microglial cells using various substrates in ACSF media. MTT viability was determined as described in Materials and Methods.

Cells incubated in ACSF were used as starving controls. MEM and DMEM indicate conditions, where cells were incubated in culture media. Data are presented as means of 18-24 replicates from 3 individual experiments \pm SEM * $P = <0,001$ versus ACSF control evaluated by one-way ANOVA.

3.4 Effect of energy substrates on cell apoptosis and necrosis

Apoptotic primary and BV-2 microglial cells were detected by double labelling with Annexin V-352 Cy3.18 and calcein-AM as described in the Materials and Methods. Cells stained only with Annexin V were considered necrotic cells, which exhibited the loss of plasma membrane integrity. Starvation for four hours in ACSF did not induce apoptosis or necrosis in primary microglia; 95-99 % of these cells were only labelled with calcein, which reflects their viability, and a small portion (1-5 %) were considered apoptotic or necrotic cells. For the positive control, 400 μ M H_2O_2 were administered to the cellular media. The portion of calcein-positive vital cells was decreased to 50% and the percentages of apoptotic and necrotic cells were increased to 25 – 25 % following exposure to H_2O_2 (Fig. 8A).

Starvation had a major impact on apoptosis induction in BV-2 cells. The proportion of calcein-positive cells was decreased to less than 60% following starvation in the nutrient-free ACSF. However, approximately 90% of the cells remained viable in the presence of glutamine (Fig. 8B). Other respiratory substrates were unable to increase the viability of the BV-2 cells.

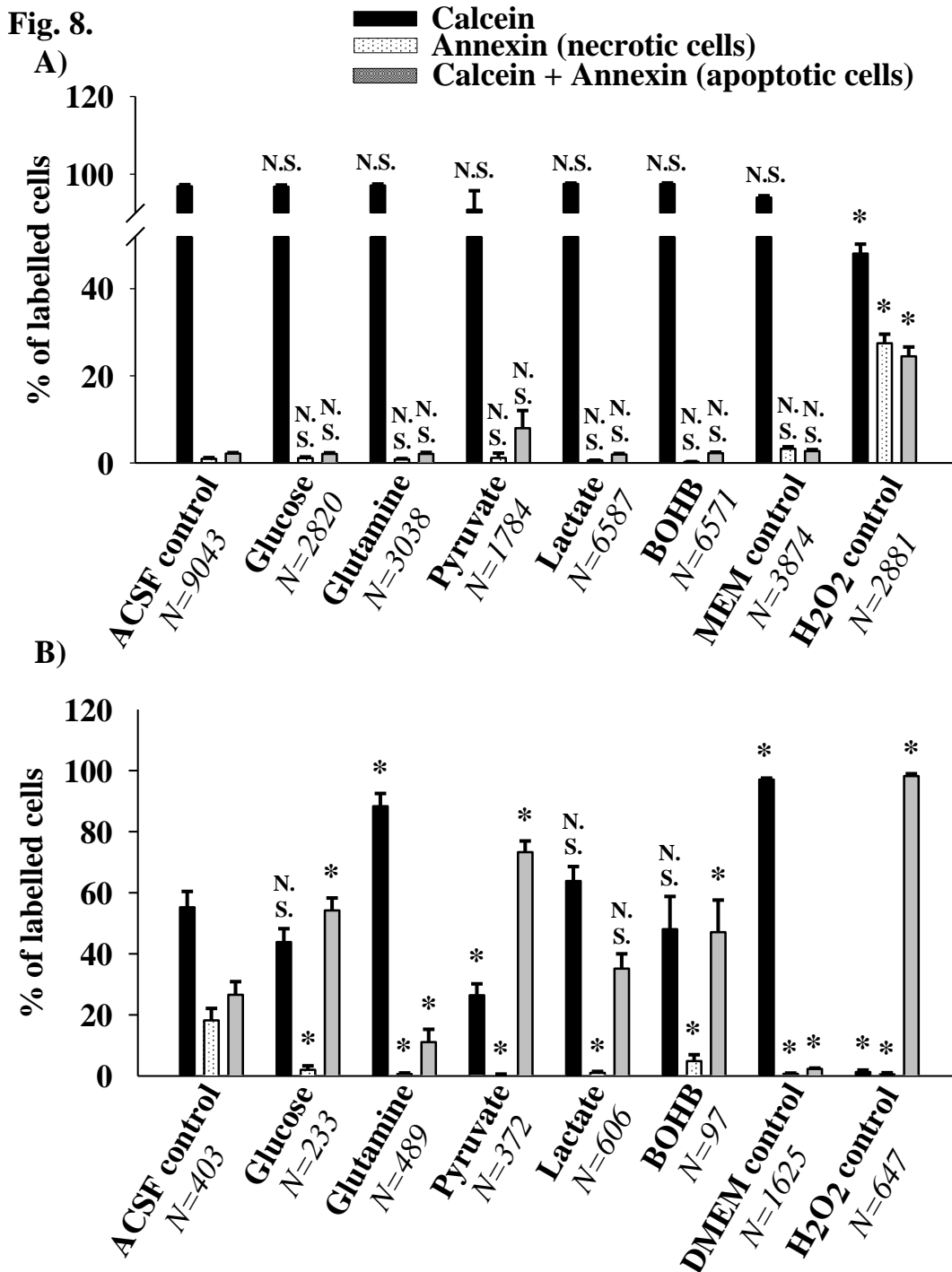


Fig. 8. Induction of apoptotic and necrotic cell death in primary (A) - and BV-2 (B) microglial cells upon starvation. Apoptotic and necrotic cells were visualized by Annexin V - Cy3.18/ calcein-AM double staining as detailed in Materials and Methods. *N* reflects the number of detected cells. 100 % is the total number of analyzed cells in each condition. Cells incubated in ACSF were used as starving controls. MEM and DMEM indicate conditions, where cells were incubated in culture

media. * $P = <0,001$ indicate statistically significant difference versus ACSF control evaluated by one-way ANOVA analysis.

3.5 Effect of energy substrates on the mTOR phosphorylation, AMPK phosphorylation and p-S6 level

The cytoplasmatic protein complex mammalian target of rapamycin C1 (mTORC1) is an essential member in the tight coupling of growth promoting signals and anabolic processes. Studies have demonstrated that lack of amino acids results in a block of the mTORC1 (Sancak *et al.* 2008, Bar-Peled *et al.* 2012). It has recently been elucidated that a lysosomal transporter SLC38A9 acts as a molecular sensor of amino acids, such as glutamine and arginine, and it activates/represses the mTOR kinase (Rebsamen *et al.* 2015, Wang *et al.* 2015). To investigate the effect of glutamine on mTOR phosphorylation, we performed immunoblot experiments to determine the p-mTOR/t-mTOR ratio. In parallel with that the energy sensing hunger signal protein kinase AMPK phosphorylated (p-AMPK, active) and total (t-AMPK) forms were also detected. Following phosphorylation, the mTORC1 regulates protein synthesis *via* S6 kinase. Therefore, the p-S6 levels of BV-2 cells were measured via FACS analysis with glucose or glutamine as a substrate. In the nutrient-free ACSF media, reduced levels of p-S6 and the p-mTOR/t-mTOR ratio were identified compared with the DMEM control cells, which indicates a starvation-evoked decrease in protein synthesis. However, the p-S6 expression level was only partially restored by glutamine in the BV-2 microglial cells (Fig. 9 and 10). The p-AMPK/t-AMPK ratio was elevated in starving and glucose-treated cells compared with the cells supplemented with glutamine or DMEM, however, the difference was not significant. (Fig. 10B.).

Fig. 9.

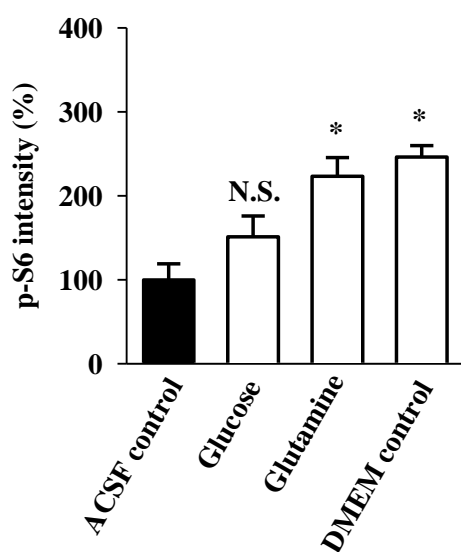


Fig. 9. The effects of glucose and glutamine on the level of p-S6 in BV-2 microglial cells. Anti-p-S6 staining intensity was measured by flow cytometry as detailed in Materials and Methods. Values represent the means \pm SEM for 3 independent experiments * P = 0,002 indicates statistically significant difference versus ACSF control evaluated by one-way ANOVA followed.

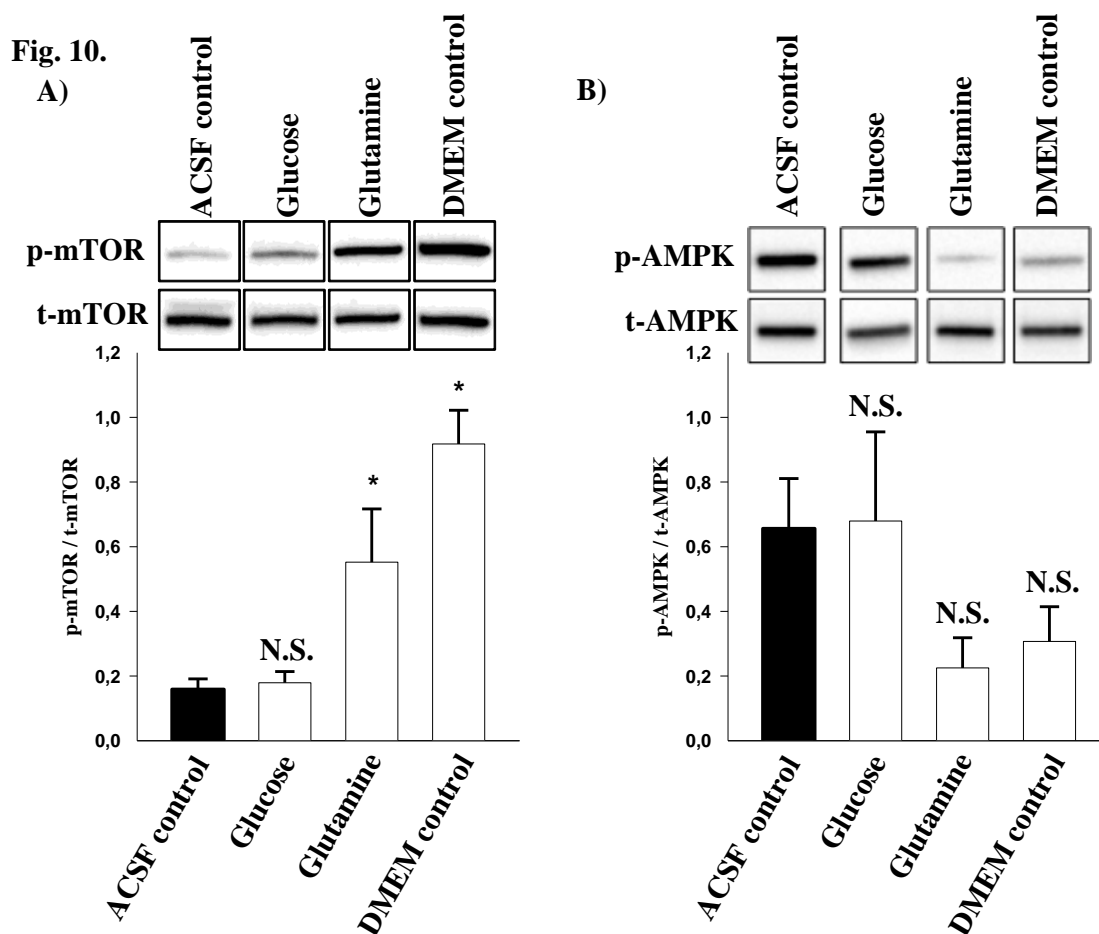


Fig. 10. Effect of energy substrates on mTOR (A) and AMP kinase (AMPK) (B) signaling system of BV-2 microglial cells. The phosphorylated mTOR (p-mTOR), total-mTOR (t-mTOR) and the phosphorylated AMPK (p-AMPK, active), and total-AMPK (t-AMPK) intensities were measured by Western-blot analysis as defined in Materials and Methods. The phosphorylated/total ratio was calculated from the densitometric results. Bars represent the mean values of at least 3 independent experiments \pm SEM. * P = <0,001 indicates statistically significant difference versus ACSF control evaluated by one-way ANOVA.

3.6 Effect of energy substrates on the autophagic activity

The formation of autophagosomes is highly inducible. Nutrient deprivation, particularly the lack of amino acids, is proposed to be a major inducer of autophagy through mTORC1 suppression (Shibutani & Yoshimori 2014, Singh & Cuervo 2011). The ratio of the phosphatidylethanolamine-

conjugated LC3 (LC3 II) and the phosphatidylethanolamine-unconjugated LC3 (LC3 I) correlates well with the number of autophagosomes/autolysosomes; thus, it is widely used as a marker of autophagy (Kabeya *et al.* 2000, Klionsky *et al.* 2012). In the present study, the expression levels of LC3 II and LC3 I proteins were assessed under various substrate conditions. The LC3 II/I ratio was significantly increased in the BV-2 cells following starvation for four hours in ACSF compared with the DMEM control cells. However, in the presence of glutamine, the autophagic activity was decreased compared with the starving cells (Fig. 11).

Fig. 11.

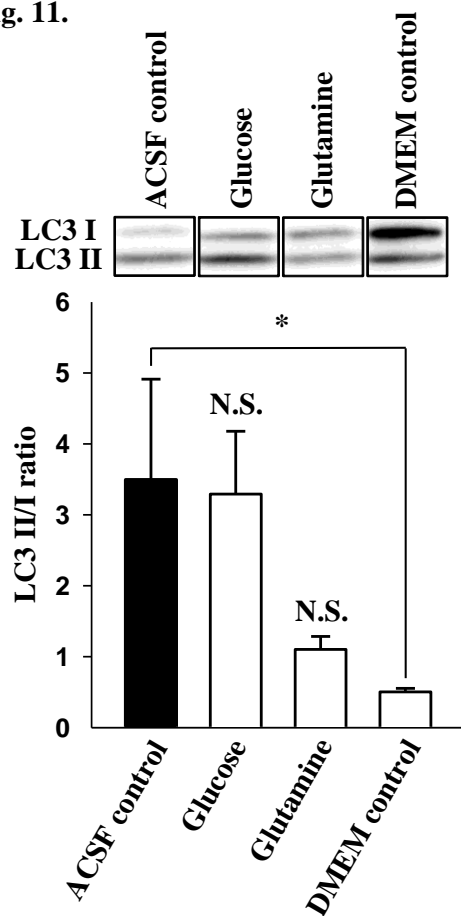


Fig. 11. Effect of energy substrates on the autophagic activity of BV-2 microglial cells. LC3 II/I ratio was determined by Western-blot analysis as detailed in Materials and Methods. Data are presented as means of at least 3 individual experiments \pm SEM * $P = 0,012$ versus ACSF control evaluated by one-way ANOVA.

4. Discussion

The distribution of microglia in the adult, healthy brain is heterogeneous (Lawson *et al.* 1990). Microglia migrate into different brain regions (for review, refer to (Kettenmann *et al.* 2011)), where they encounter various metabolic conditions. The available energy substrates in these brain microcompartments determine the metabolic route of microglial energy production. Many studies indicate that these cells in the surveillance state are more dependent on oxidative compared with glycolytic metabolism (Cherry *et al.* 2014, Orihuela *et al.* 2015, Voloboueva *et al.* 2013). However, the exact specification of substrate utilization remains to be elucidated.

To our knowledge, the energy substrate preference of microglia in the resting state has not been directly investigated. *In vitro* studies were performed on primary microglial cultures and BV-2 microglial cells under energy-deprived conditions. In the absence of energy substrates, both primary and BV-2 cells exhibited decreases in the basal oxygen consumption and a reduced maximal respiration (Table 1A and 1B) with a decrease in the intracellular ATP levels (Fig. 6A and 6B), indicating a serious energy deficit. In primary microglia, in contrast to BV-2 cells starvation did not decrease the viability and did not significantly increase the apoptotic frequency (Fig. 7A, 8A, 7B, 8B). In BV-2 cells m-TOR phosphorylation activity was reduced in starvation (Fig. 9-10), indicating a decrease in the rate of protein synthesis (Morita *et al.* 2015). The increased LC3 II/I ratio is consistent with the initiation of self-degradative processes (Kabeya *et al.* 2000) (Fig. 11). It is concluded that in term of viability primary microglial cells are less sensitive to nutrient deprivation than cells of BV-2 cell line.

To investigate the substrate utilization, cells were maintained in ACSF medium supplemented with different glycolytic or oxidative substrate. Energy metabolites selected for this study are present in the CSF under physiological conditions (Albrecht *et al.* 2007, Leen *et al.* 2012, Zhang & Natowicz 2013). Oxygen consumption data in the presence or absence of exogenous energy substrates are depicted in Table 1A and B. However, it is assumed that oxygen consumption in the presence of exogenous substrates may be a sum of oxidation of the endogenous plus exogenous substrates. Therefore, to find net contribution of exogenous substrate to OCR basal ACSF rates were be subtracted from ACSF + substrate rates (Table 2A and 2B.).

The respiration quotient is close to 1 for the brain (cortex), which indicates aerobic oxidation of glucose (Dickens 1936, Krebs 1964, Cahill & Owen 1967, Stiles & Lusk 1903). In our experiments, the administration of glucose decreased oxygen consumption in both cell types (Table 1A and 1B). This acute effect of glucose is similar to that identified in cancer cells (Crabtree 1929, Warburg 1956) and in NE-4C stem cells (Jady *et al.* 2016) that are mainly dependent on glycolysis. However,

the oligomycin induced decrease in OCR indicated the function of oxidative phosphorylation (Table 1A and 1B). Glucose highly stimulated the rate of acidification of the extracellular medium, indicating the increased rate of glycolysis (Fig. 2B, 2D, 3B, 3D). The results suggest a possible metabolic cooperation between microglia and neuron, lactate produced by microglia could support neuronal oxidative metabolism.

Glucose partially preserved the ATP level in primary microglial cells but not in BV-2 cells. Moreover, glucose did not stimulate survival and did not decrease the apoptotic frequency in BV-2 cells (Fig. 7B, 8B). Glucose was also not efficient to protect against the increased rate of autophagy (Fig. 11) and was unable to stimulate the phosphorylation of mTOR (Fig. 10); thus, it could not reverse the starvation induced catabolic pathways in BV-2 microglial cells. The possible reasons for the inhibition of the oxidative metabolism of glucose were also investigated. The results presented in Table 1A and 1B indicate that the low level of pyruvate dehydrogenase complex activity (PDHc) could not be responsible for the low rate of oxidative metabolism; i) the addition of uncoupler augmented the rate of respiration in primary microglia, ii) inhibition of lactate dehydrogenase by oxamate (Novoa *et al.* 1959) stimulated the entry of glycolytic pyruvate into mitochondria, increased cellular respiration and decreased the rate of acidification in both primary and BV-2 microglial cells (Fig. 1A-D). It is concluded that ATP production *via* glycolysis may maintain PDHc in a partially inactivated state however, uncoupling or increasing the substrate concentration may overcome this.

When glucose was replaced by pyruvate (Table 1A and 1B, rows b and d), ATP could not be produced in glycolysis; therefore, to produce ATP, pyruvate should enter into the TCA cycle. This need for ATP may activate PDHc enzymes in primary microglial cells. Pyruvate-supported oxidation significantly enhanced the cellular ATP levels in primary cells. However, this effect was not identified in BV-2 microglial cells. In accordance with this finding, pyruvate did not increase cell viability, as measured by MTT (Fig. 7B), and did not decrease the percentage of apoptotic cells (Fig. 8B).

Lactate is a proven physiologic substrate in the CNS (Rinholm & Bergersen 2014). The astrocytic production and neuronal consumption of lactate are well documented (Belanger *et al.* 2011, Magistretti & Allaman 2015). Primary and BV-2 microglial cells utilized lactate and exhibited an increased rate of basal and maximal respiration (Table 1A and 1B). ATP levels of the primary microglial cells were also significantly increased in the presence of lactate compared with the ACSF controls (Fig. 6). Although lactate is an effective oxidative substrate for BV-2 cells, the ATP and MTT results demonstrate that these cells were not able to preserve their ATP levels and viability in the presence of lactate (Fig. 6 and 7). It is interesting to compare the effects of lactate

and pyruvate on oxygen consumption. In primary microglial cells, both the basal and the maximal OCR were more stimulated by pyruvate than by lactate (Table 1, Row b). One potential explanation may be that pyruvate may enter into mitochondria and directly serve as a substrate for PDHc, whereas lactate should first be oxidized by lactate dehydrogenase (LDH). NADH, formed in the reaction catalysed by LDH, ought to enter into mitochondria using shuttle mechanisms because the cytosolic NADH utilizing capacity is low. In starving cells, an insufficient function of shuttles may prevent the oxidation of lactate (Wang *et al.* 2015).

Glutamine is an abundant amino acid in the brain (McGale *et al.* 1977) and is part of the glutamate-glutamine cycle (Albrecht *et al.* 2007). It comprises a relevant energy metabolite for cancer cells (Seyfried *et al.* 2015), as well as for lymphocytes, macrophages and neutrophil granulocytes (Newsholme 2001). Here, we demonstrate that under starving conditions, the basal respiration is increased by the addition of glutamine as a single metabolic fuel, and the glutamine-induced oxygen-consumption is associated with ATP synthesis in primary and BV-2 microglial cells. Uncoupled respiration, which demonstrates a maximal utilization of the substrate, was clearly the highest in BV-2 cells when glutamine was present in the ACSF (Table 1B). BV-2 cells exhibited a high ATP/ADP ratio and maintained the MTT viability in the presence of glutamine (Fig. 6B and 7B). Significantly increased mTOR activity and p-S6 levels were observed in the presence of glutamine that suggest an increased rate of protein synthesis compared with the ACSF control cells (Fig. 9-10.). Although there was not a significant difference between glutamine-treated and starving (ACSF only) BV-2 cells concerning the p-AMPK/t-AMPK, and the LC3 II/I ratios, respectively, but the tendencies were obvious, the well established reciprocal regulation (for review see (Wong *et al.* 2013)) between mTOR and autophagy, furthermore between AMPK and mTOR was justified in the present study as well (Figures 9-11). Glutamine reversed the general catabolic pattern of microglial cells.

It is proposed that microglia can participate in the glutamate-glutamine cycle and could buffer not only glutamate (Persson *et al.* 2006), but also glutamine in the CSF.

It seemed to be obvious to investigate the role of glutamate as a metabolic fuel for microglial cells, however the expression of wide range of glutamate receptors (Kettenmann *et al.* 2011) would have made the distinction between the metabolic and the receptor-mediated effects very difficult.

Beta-hydroxybutyrate and acetoacetate (ketone bodies) may also serve as effective energy substrates for microglia in starvation. In the present study, we demonstrated that the basal and maximal levels of respiration were increased in the presence of BOHB. However, this increase was the lowest among the substrates (Table 1A and 1B).

To further characterize the role of ketone bodies in microglial metabolism, another ketone body, acetoacetate, was added to microglia. In the absence of glutamine, acetoacetate did not significantly influence the basal level of oxidation; however, it transiently stimulated the maximal rate of respiration (Fig. 4). When glutamine was present in the media, acetoacetate maintained a long-lasting stimulation of oxygen consumption. It is concluded that in starvation, the oxidation of ketone bodies is seriously limited by the low availability of succinyl-CoA. This finding is reflected in the fast decline of acetoacetate oxidation. In glutamine-supported microglia, the flux of oxidized intermediates of glutamine metabolism likely generates sufficient succinyl-CoA to support ketone body metabolism (Fig. 4). These findings indicate that starvation of microglial cells resulted in a depletion of TCA-cycle intermediates, which hampered the oxidation of ketone bodies; however, with a proper combination of substrates, the cycle function may be improved. It could be proposed that microglial cells *in vivo* is likely utilize ketone bodies produced by the liver or by astrocytes.

Another substrate combination proved to be efficient to stimulate respiration of BV-2 cells. Aspartate pre-treatment stimulated the oxidation of glucose, pyruvate and lactate (Fig. 5A-D). From these experiments it can be concluded that there is a relatively high transamination capacity in these cells to create acetyl-CoA acceptor oxaloacetate from aspartate. It is important to point out that although both aspartate and malate did significantly augment the maximal respiration of glucose, but the basic phenomenon the suppression of endogenous respiration by glucose (Warburg-like effect) has not been changed.

Our results first demonstrate the remarkable metabolic flexibility of microglial cells, using a wide range of substrates potentially present in the cerebrospinal fluid. This plasticity may help these cells to adapt their energy homeostasis to different metabolic compartments in the brain. Of the various substrates suitable to provide energy for microglial cells, glutamine plays a prominent role. Thus, microglia may function as a potential regulator of the glutamate/glutamine pool. We also propose the possibility of metabolic cooperation between microglia, neurons and astrocytes that contribute to the balanced energy supply of various CNS cell types. These findings form a basis for functional studies *in vivo*, with the aim of identifying the contribution of microglia to brain energy metabolism.

5. Acknowledgements

This work was supported by grants from the Hungarian Brain Research Program (KTIA_13_NAP-A-III/6), National Science Foundation (OTKA NK 81983), Social Renewal Operational Programme (TÁMOP 4.2.2./B-09/1), Hungarian Academy of Sciences (MTA TKI 2013) to VAV. The authors are indebted to Mrs. Katalin Zolde for excellent technical assistance and to Dr. Tunde Kovacs for her valuable help in experiments and evaluations. The authors declare no competing financial interests.

ACCEPTED MANUSCRIPT

6. References

- Albrecht, J., Sonnewald, U., Waagepetersen, H. S. and Schousboe, A. (2007) Glutamine in the central nervous system: function and dysfunction. *Frontiers in bioscience : a journal and virtual library*, **12**, 332-343.
- Bar-Peled, L., Schweitzer, L. D., Zoncu, R. and Sabatini, D. M. (2012) Ragulator is a GEF for the rag GTPases that signal amino acid levels to mTORC1. *Cell*, **150**, 1196-1208.
- Belanger, M., Allaman, I. and Magistretti, P. J. (2011) Brain energy metabolism: focus on astrocyte-neuron metabolic cooperation. *Cell metabolism*, **14**, 724-738.
- Benjamin, A. M. and Quastel, J. H. (1974) Fate of L-glutamate in the brain. *Journal of neurochemistry*, **23**, 457-464.
- Bessis, A., Bechade, C., Bernard, D. and Roumier, A. (2007) Microglial control of neuronal death and synaptic properties. *Glia*, **55**, 233-238.
- Blazquez, C., Woods, A., de Ceballos, M. L., Carling, D. and Guzman, M. (1999) The AMP-activated protein kinase is involved in the regulation of ketone body production by astrocytes. *Journal of neurochemistry*, **73**, 1674-1682.
- Bozyczko-Coyne, D., McKenna, B. W., Connors, T. J. and Neff, N. T. (1993) A rapid fluorometric assay to measure neuronal survival in vitro. *J Neurosci Methods*, **50**, 205-216.
- Cahill, G. F., Jr. and Owen, O. E. (1967) Some observations on carbohydrate metabolism in man. In: *Carbohydrate Metabolism and its Disorders*, (F. Dickens, P. J. Randle and W. J. Whelan eds.), pp. 497-522. Academic Press Inc., New York.
- Chakraborty, G., Mekala, P., Yahya, D., Wu, G. and Ledeen, R. W. (2001) Intraneuronal N-acetylaspartate supplies acetyl groups for myelin lipid synthesis: evidence for myelin-associated aspartoacylase. *Journal of neurochemistry*, **78**, 736-745.
- Cherry, J. D., Olschowka, J. A. and O'Banion, M. K. (2014) Are "resting" microglia more "m2"? *Front Immunol*, **5**, 594.
- Crabtree, H. G. (1929) Observations on the carbohydrate metabolism of tumours. *The Biochemical journal*, **23**, 536-545.
- Davalos, D., Grutzendler, J., Yang, G., Kim, J. V., Zuo, Y., Jung, S., Littman, D. R., Dustin, M. L. and Gan, W. B. (2005) ATP mediates rapid microglial response to local brain injury in vivo. *Nature neuroscience*, **8**, 752-758.
- De Biase, L. M., Schuebel, K. E., Fusfeld, Z. H. et al. (2017) Local Cues Establish and Maintain Region-Specific Phenotypes of Basal Ganglia Microglia. *Neuron*, **95**, 341-356 e346.

- Dickens, F. (1936) Metabolism of normal and tumour tissue: The respiratory quotient of brain cortex. *The Biochemical journal*, **30**, 661-664.
- Dringen, R., Wiesinger, H. and Hamprecht, B. (1993) Uptake of L-lactate by cultured rat brain neurons. *Neuroscience letters*, **163**, 5-7.
- Engl, E., Jolivet, R., Hall, C. N. and Attwell, D. (2017) Non-signalling energy use in the developing rat brain. *Journal of cerebral blood flow and metabolism : official journal of the International Society of Cerebral Blood Flow and Metabolism*, **37**, 951-966.
- Flowers, A., Bell-Temin, H., Jalloh, A., Stevens, S. M., Jr. and Bickford, P. C. (2017) Proteomic analysis of aged microglia: shifts in transcription, bioenergetics, and nutrient response. *Journal of neuroinflammation*, **14**, 96.
- Gerencser, A. A., Neilson, A., Choi, S. W., Edman, U., Yadava, N., Oh, R. J., Ferrick, D. A., Nicholls, D. G. and Brand, M. D. (2009) Quantitative microplate-based respirometry with correction for oxygen diffusion. *Analytical chemistry*, **81**, 6868-6878.
- Gimeno-Bayon, J., Lopez-Lopez, A., Rodriguez, M. J. and Mahy, N. (2014) Glucose pathways adaptation supports acquisition of activated microglia phenotype. *Journal of neuroscience research*, **92**, 723-731.
- Gosselin, D., Skola, D., Coufal, N. G. et al. (2017) An environment-dependent transcriptional network specifies human microglia identity. *Science*, **356**.
- Grabert, K., Michoel, T., Karavolos, M. H., Clohisey, S., Baillie, J. K., Stevens, M. P., Freeman, T. C., Summers, K. M. and McColl, B. W. (2016) Microglial brain region-dependent diversity and selective regional sensitivities to aging. *Nature neuroscience*, **19**, 504-516.
- Izumi, Y., Ishii, K., Katsuki, H., Benz, A. M. and Zorumski, C. F. (1998) beta-Hydroxybutyrate fuels synaptic function during development. Histological and physiological evidence in rat hippocampal slices. *The Journal of clinical investigation*, **101**, 1121-1132.
- Jady, A. G., Nagy, A. M., Kohidi, T., Ferenczi, S., Tretter, L. and Madarasz, E. (2016) Differentiation-Dependent Energy Production and Metabolite Utilization: A Comparative Study on Neural Stem Cells, Neurons, and Astrocytes. *Stem Cells Dev*, **25**, 995-1005.
- Kabeya, Y., Mizushima, N., Ueno, T., Yamamoto, A., Kirisako, T., Noda, T., Kominami, E., Ohsumi, Y. and Yoshimori, T. (2000) LC3, a mammalian homologue of yeast Apg8p, is localized in autophagosome membranes after processing. *EMBO J*, **19**, 5720-5728.
- Kettenmann, H., Hanisch, U. K., Noda, M. and Verkhratsky, A. (2011) Physiology of microglia. *Physiological reviews*, **91**, 461-553.
- Klionsky, D. J., Abdalla, F. C., Abeliovich, H. et al. (2012) Guidelines for the use and interpretation of assays for monitoring autophagy. *Autophagy*, **8**, 445-544.

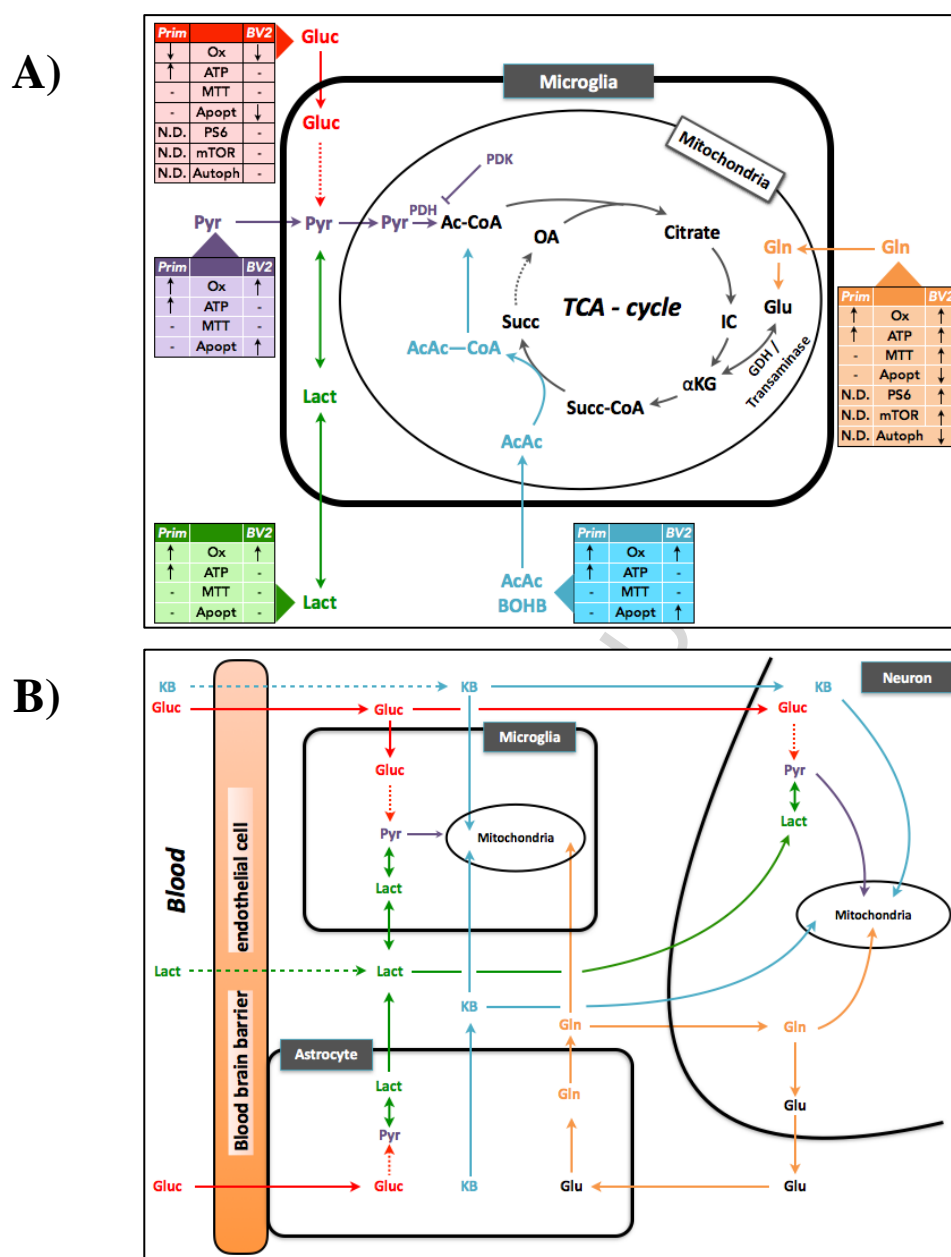
- Krebs, H. A. (1964) The metabolic fate of amino acids. In: *Mammalian Protein Metabolism*, (H. N. Muro and J. B. Allison eds.), pp. 1:125. Academic Press Inc., New York.
- Lawson, L. J., Perry, V. H., Dri, P. and Gordon, S. (1990) Heterogeneity in the distribution and morphology of microglia in the normal adult mouse brain. *Neuroscience*, **39**, 151-170.
- Leen, W. G., Willemsen, M. A., Wevers, R. A. and Verbeek, M. M. (2012) Cerebrospinal fluid glucose and lactate: age-specific reference values and implications for clinical practice. *PloS one*, **7**, e42745.
- Liddelow, S. A., Guttenplan, K. A., Clarke, L. E. et al. (2017) Neurotoxic reactive astrocytes are induced by activated microglia. *Nature*, **541**, 481-487.
- Lundin, A., Hasenson, M., Persson, J. and Pousette, A. (1986) Estimation of biomass in growing cell lines by adenosine triphosphate assay. *Methods in enzymology*, **133**, 27-42.
- Magistretti, P. J. and Allaman, I. (2015) A cellular perspective on brain energy metabolism and functional imaging. *Neuron*, **86**, 883-901.
- McGale, E. H., Pye, I. F., Stonier, C., Hutchinson, E. C. and Aber, G. M. (1977) Studies of the inter-relationship between cerebrospinal fluid and plasma amino acid concentrations in normal individuals. *Journal of neurochemistry*, **29**, 291-297.
- Michell-Robinson, M. A., Touil, H., Healy, L. M., Owen, D. R., Durafourt, B. A., Bar-Or, A., Antel, J. P. and Moore, C. S. (2015) Roles of microglia in brain development, tissue maintenance and repair. *Brain : a journal of neurology*, **138**, 1138-1159.
- Miyamoto, A., Wake, H., Ishikawa, A. W. et al. (2016) Microglia contact induces synapse formation in developing somatosensory cortex. *Nat Commun*, **7**, 12540.
- Morita, M., Gravel, S. P., Hulea, L., Larsson, O., Pollak, M., St-Pierre, J. and Topisirovic, I. (2015) mTOR coordinates protein synthesis, mitochondrial activity and proliferation. *Cell Cycle*, **14**, 473-480.
- Mosmann, T. (1983) Rapid colorimetric assay for cellular growth and survival: application to proliferation and cytotoxicity assays. *Journal of immunological methods*, **65**, 55-63.
- Nemeth, B., Doczi, J., Csete, D. et al. (2015) Abolition of mitochondrial substrate-level phosphorylation by itaconic acid produced by LPS-induced Irg1 expression in cells of murine macrophage lineage. *FASEB journal : official publication of the Federation of American Societies for Experimental Biology*.
- Newsholme, P. (2001) Why is L-glutamine metabolism important to cells of the immune system in health, postinjury, surgery or infection? *The Journal of nutrition*, **131**, 2515S-2522S; discussion 2523S-2514S.

- Nijland, P. G., Michailidou, I., Witte, M. E. et al. (2014) Cellular distribution of glucose and monocarboxylate transporters in human brain white matter and multiple sclerosis lesions. *Glia*, **62**, 1125-1141.
- Nimmerjahn, A., Kirchhoff, F. and Helmchen, F. (2005) Resting microglial cells are highly dynamic surveillants of brain parenchyma in vivo. *Science*, **308**, 1314-1318.
- Novoa, W. B., Winer, A. D., Glaid, A. J. and Schwert, G. W. (1959) Lactic dehydrogenase. V. Inhibition by oxamate and by oxalate. *The Journal of biological chemistry*, **234**, 1143-1148.
- Orihuela, R., McPherson, C. A. and Harry, G. J. (2015) Microglial M1/M2 polarization and metabolic states. *British journal of pharmacology*.
- Owen, O. E., Morgan, A. P., Kemp, H. G., Sullivan, J. M., Herrera, M. G. and Cahill, G. F., Jr. (1967) Brain metabolism during fasting. *The Journal of clinical investigation*, **46**, 1589-1595.
- Paolicelli, R. C., Bolasco, G., Pagani, F. et al. (2011) Synaptic pruning by microglia is necessary for normal brain development. *Science*, **333**, 1456-1458.
- Pellerin, L. and Magistretti, P. J. (1994) Glutamate uptake into astrocytes stimulates aerobic glycolysis: a mechanism coupling neuronal activity to glucose utilization. *Proceedings of the National Academy of Sciences of the United States of America*, **91**, 10625-10629.
- Peng, L., Zhang, X. and Hertz, L. (1994) High extracellular potassium concentrations stimulate oxidative metabolism in a glutamatergic neuronal culture and glycolysis in cultured astrocytes but have no stimulatory effect in a GABAergic neuronal culture. *Brain research*, **663**, 168-172.
- Persson, M., Sandberg, M., Hansson, E. and Ronnback, L. (2006) Microglial glutamate uptake is coupled to glutathione synthesis and glutamate release. *The European journal of neuroscience*, **24**, 1063-1070.
- Rebsamen, M., Pochini, L., Stasyk, T. et al. (2015) SLC38A9 is a component of the lysosomal amino acid sensing machinery that controls mTORC1. *Nature*, **519**, 477-481.
- Rinholm, J. E. and Bergersen, L. H. (2014) White matter lactate--does it matter? *Neuroscience*, **276**, 109-116.
- Sancak, Y., Peterson, T. R., Shaul, Y. D., Lindquist, R. A., Thoreen, C. C., Bar-Peled, L. and Sabatini, D. M. (2008) The Rag GTPases bind raptor and mediate amino acid signaling to mTORC1. *Science*, **320**, 1496-1501.
- Sandiego, C. M., Gallezot, J. D., Lim, K., Ropchan, J., Lin, S. F., Gao, H., Morris, E. D. and Cosgrove, K. P. (2015) Reference region modeling approaches for amphetamine challenge studies with [¹¹C]FLB 457 and PET. *Journal of cerebral blood flow and metabolism :*

- official journal of the International Society of Cerebral Blood Flow and Metabolism*, **35**, 623-629.
- Saura, J., Tusell, J. M. and Serratos, J. (2003) High-yield isolation of murine microglia by mild trypsinization. *Glia*, **44**, 183-189.
- Schafer, D. P., Lehrman, E. K., Kautzman, A. G. et al. (2012) Microglia sculpt postnatal neural circuits in an activity and complement-dependent manner. *Neuron*, **74**, 691-705.
- Schilling, T. and Eder, C. (2004) A novel physiological mechanism of glycine-induced immunomodulation: Na⁺-coupled amino acid transporter currents in cultured brain macrophages. *The Journal of physiology*, **559**, 35-40.
- Schousboe, A., Svenneby, G. and Hertz, L. (1977) Uptake and metabolism of glutamate in astrocytes cultured from dissociated mouse brain hemispheres. *Journal of neurochemistry*, **29**, 999-1005.
- Schousboe, A., Westergaard, N., Sonnewald, U., Petersen, S. B., Yu, A. C. and Hertz, L. (1992) Regulatory role of astrocytes for neuronal biosynthesis and homeostasis of glutamate and GABA. *Progress in brain research*, **94**, 199-211.
- Schurr, A., West, C. A. and Rigor, B. M. (1988) Lactate-supported synaptic function in the rat hippocampal slice preparation. *Science*, **240**, 1326-1328.
- Seyfried, T. N., Flores, R., Poff, A. M., D'Agostino, D. P. and Mukherjee, P. (2015) Metabolic therapy: a new paradigm for managing malignant brain cancer. *Cancer Lett*, **356**, 289-300.
- Shibutani, S. T. and Yoshimori, T. (2014) A current perspective of autophagosome biogenesis. *Cell Res*, **24**, 58-68.
- Singh, R. and Cuervo, A. M. (2011) Autophagy in the cellular energetic balance. *Cell metabolism*, **13**, 495-504.
- Stiles, P. G. and Lusk, G. (1903) On the formation of dextrose in metabolism from the end-products of a pancreatic digest of meat. *The American journal of physiology*, **9**, 380.
- Svoboda, N. and Kerschbaum, H. H. (2009) L-Glutamine-induced apoptosis in microglia is mediated by mitochondrial dysfunction. *The European journal of neuroscience*, **30**, 196-206.
- Trenkmann, M. (2017) Gene expression: Microglia - environment defines identity. *Nat Rev Genet*, **18**, 454-455.
- Vermes, I., Haanen, C., Steffens-Nakken, H. and Reutelingsperger, C. (1995) A novel assay for apoptosis. Flow cytometric detection of phosphatidylserine expression on early apoptotic cells using fluorescein labelled Annexin V. *Journal of immunological methods*, **184**, 39-51.

- Voloboueva, L. A., Emery, J. F., Sun, X. and Giffard, R. G. (2013) Inflammatory response of microglial BV-2 cells includes a glycolytic shift and is modulated by mitochondrial glucose-regulated protein 75/mortalin. *FEBS letters*, **587**, 756-762.
- Wake, H., Moorhouse, A. J., Jinno, S., Kohsaka, S. and Nabekura, J. (2009) Resting microglia directly monitor the functional state of synapses in vivo and determine the fate of ischemic terminals. *The Journal of neuroscience : the official journal of the Society for Neuroscience*, **29**, 3974-3980.
- Wang, S., Tsun, Z. Y., Wolfson, R. L. et al. (2015) Metabolism. Lysosomal amino acid transporter SLC38A9 signals arginine sufficiency to mTORC1. *Science*, **347**, 188-194.
- Warburg, O. (1956) On respiratory impairment in cancer cells. *Science*, **124**, 269-270.
- Wong, P. M., Puente, C., Ganley, I. G. and Jiang, X. (2013) The ULK1 complex: sensing nutrient signals for autophagy activation. *Autophagy*, **9**, 124-137.
- Zhang, W. M. and Natowicz, M. R. (2013) Cerebrospinal fluid lactate and pyruvate concentrations and their ratio. *Clin Biochem*, **46**, 694-697.
- Zhang, Y., Chen, K., Sloan, S. A. et al. (2014) An RNA-sequencing transcriptome and splicing database of glia, neurons, and vascular cells of the cerebral cortex. *The Journal of neuroscience : the official journal of the Society for Neuroscience*, **34**, 11929-11947.

Graphical abstract



Summary of results obtained with primary and BV-2 microglial cells (**A**) and proposed metabolic cooperation between microglia and other cell types of the brain (**B**). Abbreviations: Ox (Oxygen consumption), N.D. (not detected), – (no significant change versus ACSF control), Ac-Ac (Acetoacetate), Glu (glutamate), IC (isocitrate), α -KG (α -ketoglutarate), Succ (succinate), OA (oxaloacetate), Gluc (glucose), Gln (glutamine), Glu (glutamate), Pyr (pyruvate), Lac (lactate), KB (ketone bodies)

Highlights

In starving microglial cells (primary and BV-2):

- cellular respiration, ATP level and cell viability were decreased
- glutamine stimulated respiration and reversed most starvation-induced processes
- anaplerosis of citrate cycle enhanced ketone body oxidation

ACCEPTED MANUSCRIPT